Rod Packings and Metal−Organic Frameworks Constructed from Rod-Shaped Secondary Building Units

Nathaniel L. Rosi,[†] Jaheon Kim,[†,§] Mohamed Eddaoudi,[†,||] Banglin Chen,[†,⊥] Michael O'Keeffe,*,[‡] and Omar M. Yaghi*,[†]

Contribution from the Departments of Chemistry, University of Michigan, Ann Arbor, Michigan 48109, and Arizona State University, Tempe, Arizona 85287

Received August 12, 2004; E-mail: mokeeffe@asu.edu; oyaghi@umich.edu

Abstract: The principal structure possibilities for packing infinite rod-shaped building blocks are described. Some basic nets derived from linking simple rods (helices and ladders) are then enumerated. We demonstrate the usefulness of the concept of rod secondary building units in the design and synthesis of metal−organic frameworks (MOFs). Accordingly, we present the preparation, characterization, and crystal structures of 14 new MOFs (named MOF-69A−C and MOF-70−80) of 12 different structure types, belonging to rod packing motifs, and show how their structures are related to basic nets. The MOFs reported herein are of polytopic carboxylates and contain one of Zn, Pb, Co, Cd, Mn, or Tb. The inclusion properties of the most open members are presented as evidence that MOF structures with rod building blocks can indeed be designed to have permanent porosity and rigid architectures.

Introduction

The design and synthesis of metal−organic frameworks (MOFs) has yielded a large number of structures which have been shown to have useful gas and liquid adsorption properties.[1] In particular, porous structures constructed from discrete metal−carboxylate clusters and organic links have been shown to be amenable to systematic variation in pore size and functionality, an aspect that has led to the synthesis of MOFs capable of remarkable methane and hydrogen storage properties.[1c−f] The permanent porosity of such MOFs is imparted by the structural properties of the metal−carboxylate clusters, where each metal ion is locked into position by the carboxylates to produce rigid entities of simple geometry, referred to as secondary building units (SBUs). In the interpretation and prediction of MOF structures, the SBUs are considered as the "joints" and the organic links as the "struts" of the underlying net. MOFs based on discrete shapes (triangles, squares, tetrahedra, etc.) have been synthesized and studied. An illustrative example is MOF-5 where the metal−carboxylate structure, **a**, is an octahedral SBU
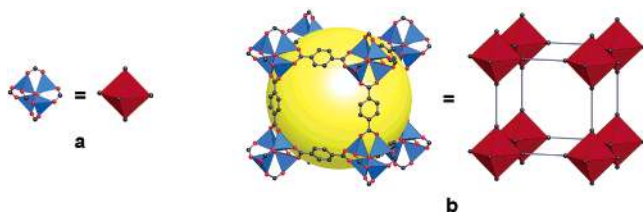
linked by benzene units to produce a primitive cubic net, **b**. Simplification of MOF structures in this way has led us to fully enumerate and describe the principal topological possibilities available for the assembly of various discrete SBU geometries.[2]

Indeed, the large majority of structural and sorption studies have been done on MOFs of discrete SBUs, yet the analogous chemistry involving infinite rod-shaped SBUs remains largely unexplored. We recently found that rod-shaped metal−carboxylate SBUs provide means to accessing MOFs that do not interpenetrate due to the intrinsic packing arrangement of such

† University of Michigan.

‡ Arizona State University.

§ Present address: Department of Chemistry and CAMDRC, Soongsil University, Seoul 156-743, Korea.

|| Present address: Department of Chemistry, University of South Florida, Tampa, FL 33620.

⊥ Present address: Department of Chemistry, University of Texas-Pan American, Edinburg, TX 78541.

(1) MOFs with porous properties: (a) Li, H.; Eddaoudi, M.; O'Keeffe, M.; Yaghi, O. M. *Nature* **1999**, *402*, 276−279. (b) Chae, H. K.; Siberio-Perez, D. Y.; Kim, J.; Go, Y.; Eddaoudi, M.; Matzger, A. J.; O'Keeffe, M.; Yaghi, O. M. *Nature* **2004**, *427*, 523−527. (c) Eddaoudi, M.; Kim, J.; Rosi, N.; Vodak, D.; Wachter, J.; O'Keeffe, M.; Yaghi, O. M. *Science* **2002**, *295*, 469−472. (d) Rosi, N. L.; Eckert, J.; Eddaoudi, M.; Vodak, D. T.; Kim, J.; O'Keeffe, M.; Yaghi, O. M. *Science* **2003**, *300*, 1127−1129. (e) Rowsell, J. L. C.; Millward, A. R.; Park, K. S.; Yaghi, O. M. *J. Am. Chem. Soc.* **2004**, *126*, 5666−5667. (f) Noro, S.; Kitagawa, S.; Kondo, M.; Seki, K. *Angew. Chem., Int. Ed.* **2000**, *39*, 2081−2084. (g) Barea, E.; Navarro, J. A. R.; Salas, J. M.; Masciocchi, N.; Galli, S.; Sironi, A. *J. Am. Chem. Soc.* **2004**, *126*, 3014−3015. (h) Serpaggi, S.; Luxbacher, T.; Cheetham, A. K.; Ferey, G. *J. Solid State Chem.* **1999**, *145*, 580−586. Chiral MOFs: (i) Cui, Y.; Evans, O. R.; Ngo, H. L.; White, P. S.; Lin, W. B. *Angew. Chem., Int. Ed.* **2002**, *41*, 1159−1162. (j) Seo, J. S.; Whang, D.; Lee, H.; Jun, S. I.; Oh, J.; Jeon, Y. J.; Kim, K. *Nature* **2000**, *404*, 982−986. (k) Kepert, C. J.; Prior, T. J.; Rosseinsky, M. J. *J. Am. Chem. Soc.* **2000**, *122*, 5158−5168. Porphyrin-containing MOFs: (l) Diskin-Posner, Y.; Dahal, S.; Goldberg, I. *Angew. Chem., Int. Ed.* **2000**, *39*, 1288−1292. (m) Carlucci, L.; Ciani, G.; Proserpio, D. M.; Porta, F. *Angew. Chem., Int. Ed.* **2003**, *42*, 317−322. (n) Kosal, M. E.; Chou, J. H.; Wilson, S. R.; Suslick, K. S. *Nat. Mater.* **2002**, *1*, 118−121. Interpenetrated MOFs: (o) Evans, O. R.; Wang, Z. Y.; Xiong, R. G.; Foxman, B. M.; Lin, W. B. *Inorg. Chem.* **1999**, *38*, 2969−2973. (p) Carlucci, L.; Ciani, G.; Macchi, P.; Proserpio, D. M. *Chem. Commun.* **1998**, *17*, 1837−1838. (q) Klein, C.; Graf, E.; Hosseini, M. W.; De Cian, A. *New J. Chem.* **2001**, *209*, 207−209. (r) Batten, S. R.; Robson, R. *Angew. Chem., Int. Ed.* **1998**, *37*, 1461−1494. Other prominent examples of MOFs: (s) Kiang, Y. H.; Gardner, G. B.; Lee, S.; Xu, Z.; Lobkovsky, E. B. *J. Am. Chem. Soc.* **1999**, *121*, 8204−8215. (t) Braga, D.; Maini, L.; Polito, M.; Mirolo, L.; Grepioni, F. *Chem.-Eur. J.* **2003**, *9*, 4362−4370. (u) Zhao, H.; Heintz, R. A.; Ouyang, X.; Dunbar, K. R.; Campana, C. F.; Rogers, R. D. *Chem. Mater.* **1999**, *11*, 736−746. (v) Cotton, F. A.; Lin, C.; Murillo, C. A. *Acc. Chem. Res.* **2001**, *34*, 759−771. (w) Oh, M.; Carpenter, G. B.; Sweigart, D. A. *Acc. Chem. Res.* **2004**, *37*, 1−11. (x) Lu, J. J.; Mondal, A.; Moulton, B.; Zaworotko, M. J. *Angew. Chem., Int. Ed.* **2001**, *40*, 2113−2116.

Table 1. Invariant Rod Packings and Their Associated Nets[a]

symbol	type	sp. gr.	[uvw]	x_0, y_0, z_0	rod group	net vertices	Z	net	d/l
1	parallel	$P6/mmm$	[001]	$^1/_3,^2/_3,0$	$p\bar{6}m2$	$^1/_3,^2/_3,0$	5	bnn	free
2	parallel	$P4/mmm$	[001]	0,0,0	$p4/mmm$	0,0,0	6	pcu	free
3	parallel	$P6/mmm$	[001]	$^1/_2,0,0$	pmmm	$^1/_2,0,0$	6	kag	free
4	parallel	$P6/mmm$	[001]	0,0,0	$p6/mmm$	0,0,0	8	hex	free
5	layers	$I4_1/amd$	[010]	0,0,0	pmcm	$0,^1/_4,0$	3	ths-z	free
6	layers	$P4_2/mmc$	[100]	0,0,0	pmmm	0,0,0	4	cds	free
7	layers	$P6_222$	[010]	$^1/_2,0,^1/_6$	$p222_1$	$^1/_2,0,^1/_6$	3	bto-z	free
8	layers	$P6_222$	[100]	0,0,0	p222	0,0,0	4	qzd	free
9Π	3-way	$I4_132$	[100]	$^1/_4,0,0$	$p4_122$	$^1/_4,0,0$	3	bmn	1
10Π*	3-way	$Pm\bar{3}n$	[100]	$^1/_2,0,0$	$p4_2/mmc$	$^1/_2,0,0$	4	nbo	1
11Σ	4-way	$I4_132$	[111]	$^1/_3,^2/_3,0$	$p3_12$	$^1/_8,^1/_{24},^7/_{24}$	3	sgn	$1/\sqrt{6}$
12Γ	4-way	$Ia\bar{3}d$	[111]	0,0,0	$p\bar{3}c$	$^1/_8,^1/_8,^1/_8$	5	gan	$\sqrt{(^2/_3)}$
13Ω	4-way	$I4\bar{3}2$	[111]	$^1/_3,^2/_3,0$	$p3_12$	$^1/_4,^5/_{12},^1/_{12}$	3	utb-z	$\sqrt{(^2/_3)}$
14Σ*	4-way	$Ia\bar{3}d$	[111]	$^1/_3,^2/_3,0$	$p3_12$	$^1/_8,^1/_{24},^7/_{24}$	3	sgn-c	$1/\sqrt{6}$

[a] Z is the coordination number of the net. Under "net" is the name of the net.[2f] The number under "symbol" corresponds to that shown in Figure 1. The rod group is the symmetry of the rod. For nets named **ths-z**, **cds**, **bto-z**, and **qzd**, $c/a = 2$, 2, $^3/_2$, 3, respectively, for equal links. Number 14 (Σ*) is two intergrown packings of number 11 (Σ). For rod symmetries, see, for example, ref 7. For net symbols, see ref 2d,e.

rods in the crystal structure.[3] In this contribution, we present strategies for the design and construction of porous structures from rod-shaped building blocks. Specifically, we (a) provide an account of the geometric principles of basic rod packing and nets based on them, (b) identify the principal topological possibilities and the most likely structures that could form from rods, (c) adduce a number of new MOFs with structures constructed according to these geometric principles, and (d) show that, similar to MOFs of discrete SBUs, MOFs based on rod SBUs can also have stable architectures and permanent porosity.

Geometric Principles of Rod Packing

A rod is a 1-periodic three-dimensional structure with a linear axis that is determined by specifying a point on the axis (x_0,y_0,z_0) and its direction $[uvw]$, **c**.[4] The special rod packings correspond to invariant line positions (i.e., special positions) in which lines (rod axes) lie along the directions of nonintersecting symmetry axes.[5] Thus, for packing of equivalent rods, it is sufficient to specify just one rod and the space group. There are 14 invariant structures, and they are so described in Table 1 and are illustrated in Figure 1.
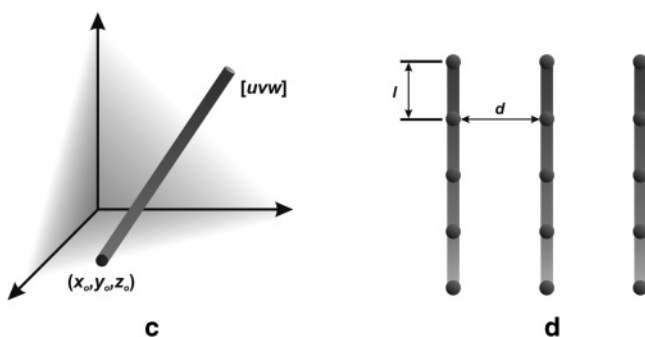
When there are points on the rod axes that join neighboring rods, then we can associate nets with each one of those rod packings. In this context, it is useful to recognize two kinds of distance: the distance between points along the rod having length *l*, and that connecting two rods having length *d*, **d**. The ratio *d/l* is an important parameter in the design of MOF structures based on rod packings, for some of which this ratio is fixed as specified in Table 1. We note that in MOF structures described here, the metal−carboxylate units (i.e., SBUs) represent the rods and the organic units link the rods together.

Simple Rod Geometries and Associated Nets

The simplest rods consist of points on a one-dimensional lattice. In the rod packings shown in Figure 1, the linear parts are rods of this kind. The next simplest rods are helices. Linking these in the simplest manner leads to 3-coordinated nets (each vertex is linked to two others on the helix and to one on a different helix) as shown in Figure 2.

For linking 3_1 or 3_2 helices, there are only two nets with one kind of vertex: one with helices of one hand and the other with helices of both hands. Wells calls them (8,3)-a and (8,3)-b, respectively;[6] in our system of naming (using a three letter code),[2d−f] they are **eta** and **etb** and they have symmetries $P6_222$ and $R\bar{3}m$, respectively (Figure 2).

4-fold helices can be similarly linked. In its most symmetrical form, the linkage of 4_1 (or 4_3) helices is cubic (symmetry $I4_132$) and corresponds to the **srs** (Si in SrSi$_2$) net [Wells' (10,3)-a][6] with three sets of nonintersecting 4_1 (or 4_3) axes. The simplest mode of linking 4_1 and 4_3 helices combined in one structure produces a tetragonal ($I4_1/amd$) structure,[6] which we label **lig** as the topology is the same as the Ge net in LiGe (Figure 2).[7]

Next in simplicity are rods of quadrangles linked by sharing opposite edges (ladders). There are two simple ways in which ladders can be linked to form 4-coordinated nets: either with the rungs parallel as in **sra** (Al net in SrAl$_2$) or at an angle to each other (**irl**) as shown in Figure 2.[8] Note that in either case the sides of the ladder form a double zigzag.[7] If successive rungs of a ladder are at right angles, one obtains a simple rod that

(2) (a) Yaghi, O. M.; O'Keeffe, M.; Ockwig, N. W.; Chae, H. K.; Eddaoudi, M.; Kim, J. *Nature* **2003**, *423*, 705−714. (b) O'Keeffe, M.; Eddaoudi, M.; Li, H.; Reineke, T. M.; Yaghi, O. M. *J. Solid State Chem.* **2000**, *152*, 3−20. (c) Eddaoudi, M.; Moler, D.; Li, H.; Chen, B.; Reineke, T. M.; O'Keeffe, M.; Yaghi, O. M. *Acc. Chem. Res.* **2001**, *34*, 319−330. (d) Delgado-Friedrichs, O.; O'Keeffe, M.; Yaghi, O. M. *Acta Crystallogr.* **2003**, *A59*, 22−27. (e) Delgado-Friedrichs, O.; O'Keeffe, M.; Yaghi, O. M. *Acta Crystallogr.* **2003**, *A59*, 515−525. (f) Crystallographic data for all structures assigned symbols in this paper are to be found at http://okeeffe-ws1.la.asu.edu/RCSR/home.htm.
(3) Rosi, N. L.; Eddaoudi, M.; Kim, J.; O'Keeffe, M.; Yaghi, O. M. *Angew. Chem., Int. Ed.* **2002**, *41*, 284−287.
(4) O'Keeffe, M.; Andersson, S. *Acta Crystallogr.* **1977**, *A33*, 914−923.
(5) O'Keeffe, M.; Plévert, J.; Watanabe, Y.; Teshima, Y.; Ogawa, T. *Acta Crystallogr.* **2001**, *A57*, 110−111.

(6) Wells, A. F. *Three-dimensional nets and polyhedra*; Wiley: New York, 1977.
(7) O'Keeffe, M.; Hyde, B. G. *Crystal Structures I: Patterns and Symmetry*; Mineral. Soc. Am.: Washington, D.C., 1996.
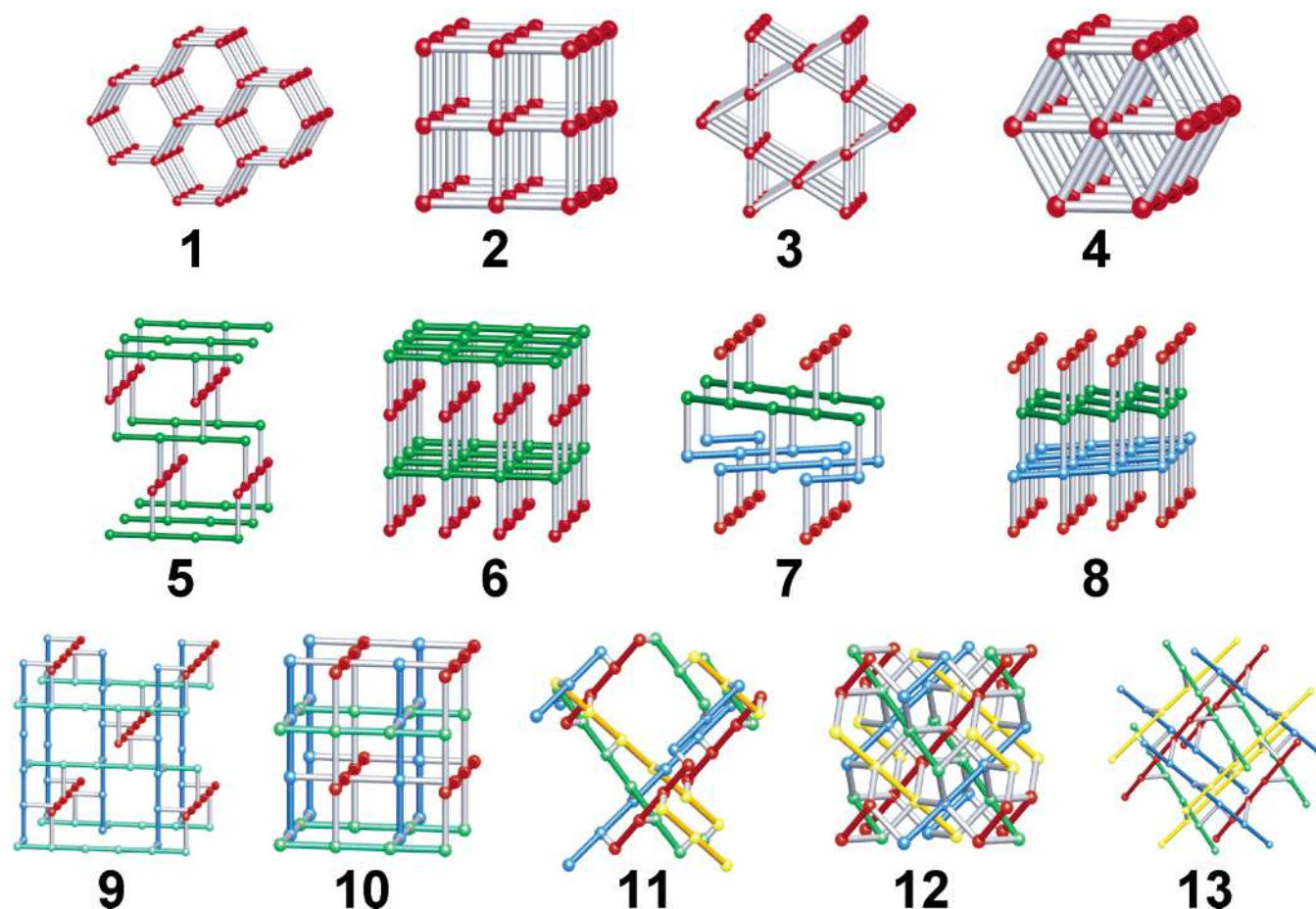(8) O'Keeffe, M. *Phys. Chem. Miner.* **1995**, *22*, 504−506.

Figure 1. Invariant rod packings. The numbers correspond to the numbers in Table 1. In 1−4, the rods are red and almost normal to the page. For 5−13, they are colored red, green, blue, and yellow.
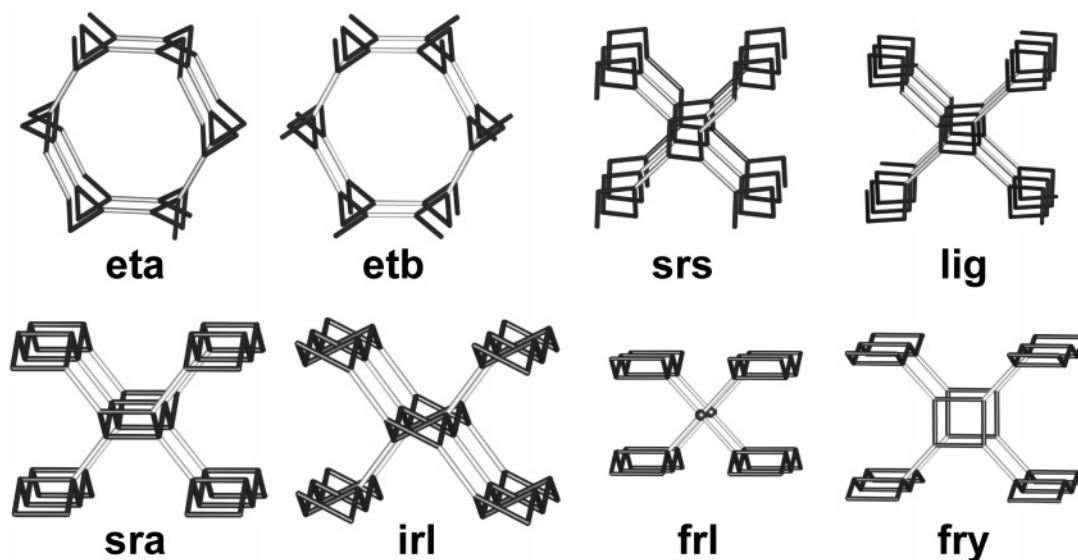

Figure 2. Nets formed by linking rods. Top row: linked helices. Bottom row left: linked ladders. Right: ladders linked to finite groups.

consists of tetrahedra sharing opposite edges, as exemplified by SiS_4 tetrahedra in SiS_2.

Rods can be combined with finite units to provide an almost endless variety of nets. We are content here just to show two simple examples of relevance to the next section that are discussed further there. These are **frl** in which zigzag ladders are joined to a point and the related partially augmented

structure, **fry**, in which the planar 4-coordinated point is replaced by a square (Figure 2).

We should note that, most commonly, linked rods will be parallel because the spacing along a rod, *l* (translation), is determined by the rod itself and the spacing between rods, *d*, is determined by the length of the links. However, if rods are not parallel, the spacing along rods and between rods may not be
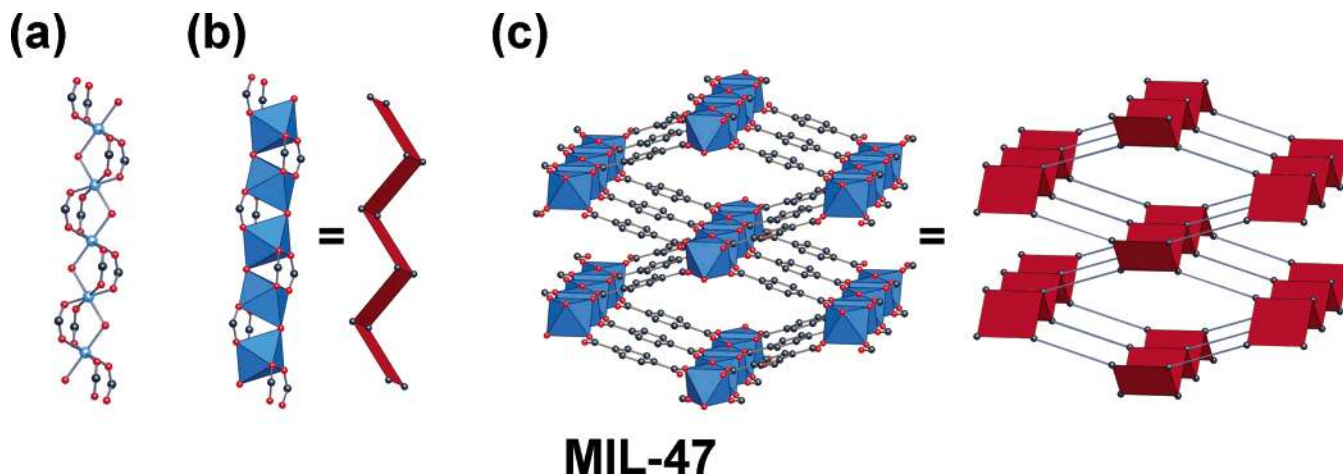
MIL-47

Figure 3. Development of the MIL-47 structure: the inorganic SBUs are chains of corner-sharing V octahedra (red = O, blue = V, black = C) (a,b) in which the carboxylate carbon atoms can be connected to form a zigzag ladder (b). When linked with organic spacers, the SBUs form crystalline frameworks that can be represented as ladders linked together as in the **sra** net (c) (Figure 2). Atomic coordinates from single-crystal data were used to produce each diagram. (Note: MIL-47 and MOF-71 are isostructural, and the crystal data for MOF-71 were used to make this diagram. For MOF-71: red = O, blue = Co, black = C.)

independent and thus a critical *d*/*l* ratio must be met to obtain the corresponding nets of **bmn**, **nbo**, **sgn**, **gan**, **utb-z**, and **sgn-c** (cf., Table 1 and Figure 1).

Recognition of Rod Secondary Building Units (SBUs)

The description of MOF geometry in terms of linked SBUs is fundamental to rationalization and prediction of MOF net topologies.[2c] Here, we refer to Figure 3 to illustrate how rod SBUs are characterized. A simple example of an infinite SBU was recently found in the structure of MIL-47 with a framework of stoichiometry VO(BDC) (BDC = 1,4-benzenedicarboxylate).[9] According to the present approach, the SBU consists of infinite $(-O-V-)_\infty$ rods (Figure 3a) with carboxylate O atoms completing octahedral coordination around V to result in an infinite rod of VO_6 octahedra sharing opposite corners (Figure 3b). The carboxylate C atoms are at the vertices of a zigzag ladder SBU. Joining the ladders through the $-C_6H_4-$ links results in a three-dimensional net of the **sra** topology (Figure 3c; cf., Figure 2). The same structure is obtained with $[-(OH)-V-]_\infty$ rods (V^{III} replacing V^{IV}). Additionally, MIL-53, consisting of $[-(OH)-(Cr)-]_\infty$[10] rods, and MOF-71 (Figure 3) (reported below), consisting of $[-O-Co-]_\infty$ rods, are both isostructural to MIL-47. The same rod appears in another structure, MIL-60,[11] in which $[-V-O-]_\infty$ rods are linked by 1,2,4,5-benzenetetracarboxylate and the topology is one of the ladder rods linked to rectangles to form a 3,4-coordinated net that we symbolize **fry** (Figure 2).[12]

In the sections that follow, we present the synthesis and characterization of MOFs constructed from rod SBUs, and we relate their underlying topologies to those of rod packing arrangements and nets.

(9) Barthelet, K.; Marrot, J.; Riou, D.; Férey, G. *Angew. Chem., Int. Ed.* **2002**, *41*, 281–284.
(10) Serre, C.; Millange, F.; Thouvenot, C.; Noguès, M.; Marsolier, G.; Louër, D.; Férey, G. *J. Am. Chem. Soc.* **2002**, *124*, 13519–13526.
(11) (a) Barthelet, K.; Riou, D.; Nogues, M.; Férey, G. *Inorg. Chem.* **2003**, *42*, 1739–1743. (b) For a related structure, see: Sanselme, M.; Grenèche, J. M.; Riou-Caveliec, M.; Férey, G. *Chem. Commun.* **2002**, 2172–2173.
(12) It is somewhat arbitrary whether we consider the anionic SBU derived from benzenetetracarboxylate as a single vertex 4-coordinated to four rods (**frl**) or as a square with each vertex linked to a rod (**fry**). The process of replacing a vertex with its coordination figure, as in the transformation **frl** → **fry**, we call augmentation, and we usually consider nets and their augmented derivatives as essentially the same topology.

Experimental Section

Synthesis and Characterization of MOFs, Abbreviations, and General Procedures. For easy reference, the formulas for MOF-69–80, explanation of guest abbreviations and organic carboxylates, and crystal unit cell parameters are listed in Table 2. Unless otherwise indicated, chemicals were purchased from the Aldrich Chemical Co. and used as received. HPDC and ATC organic linkers were synthesized according to published procedures.[13] HPDC was protected, dehydrogenated, and then deprotected to yield PDC.[14]

Elemental microanalyses were performed by The University of Michigan, Department of Chemistry, using a Perkin-Elmer CHN 2400 Series II thermal analysis system. Thermogravimetric analysis (TGA) was performed in house using a TA Q500 thermal analysis system. Fourier transform infrared (FT-IR) spectra were measured using a Nicolet FT-IR Impact 400 system. FT-IR samples were prepared as KBr pellets. Absorptions are described as follows: strong (s), medium (m), weak (w), shoulder (sh), and broad (br).

X-ray powder diffraction patterns were measured using a Bruker AXS D8 Advance powder diffractometer at 40 kV, 40 mA for Cu Kα ($\lambda = 1.5406$ Å), with a scan speed of 0.15 s/step and a step size of 0.417°. The simulated powder patterns were calculated using single-crystal X-ray diffraction data and were processed by the PowderCell 2.3 program.

The single-crystal structural determinations were done using a Bruker SMART APEX CCD diffractometer. The SMART software was used for data acquisition, SAINT for data extraction, SADABS for the absorption corrections, and SHELXTL for the structure solution and refinement. All structures were solved with direct methods. Data collection, structure solutions, and refinement, including metric parameters, have been deposited as Supporting Information.

Gas Sorption Isotherms. Sorption isotherm measurements were performed by monitoring the weight change as a function of relative pressure. Data were acquired on a CAHN 1000 electrogravimetric balance using a 1 mg scale (sensitivity 1 μg). A known weight (100–150 mg) of the as-synthesized starting material was placed in a cylindrical quartz bucket (height = 30 mm, and o.d. × i.d. = 19 × 17 mm) and was then subjected to a heating program at pressures as low as 1×10^{-5} Torr to remove the guests and produce the evacuated

(13) HPDC synthesis: (a) Connor, D. M.; Allen, S. D.; Collard, D. M.; Liotta, C. L.; Schiraldi, D. A. *J. Org. Chem.* **1999**, *64*, 6888–6890. ATC synthesis: (b) Newkome, G. R.; Nayak, A. R.; Moorefield, C.; Baker, G. *J. Org. Chem.* **1992**, *57*, 358–362.
(14) PDC was prepared using the procedure described in: Musa, A.; Sridharan, B.; Lee, H.; Mattern, D. L. *J. Org. Chem.* **1996**, *61*, 5481–5484.

Table 2. Explanation of Abbreviations for Organic Carboxylates and Guest Molecules and Crystal Unit Cell Parameters

MOF-n	Link and Abbreviation[a]	Chemical Formula[b] Space Group; a, b, c, (Å); α, β, γ (°); V (Å³); Z
MOF-69A	BPDC	$Zn_3(OH)_2(BPDC)_2 \cdot (DEF)_4(H_2O)_2$ *C2/c*; 23.1179, 20.9193, 12.0022; 90.00, 111.627, 90.00; 5395.7; 4
MOF-69B	NDC	$Zn_3(OH)_2(NDC)_2 \cdot (DEF)_4(H_2O)_2$ *C2/c*; 20.1658, 18.5518, 12.1581; 90.00, 95.331, 90.00; 4528.9; 4
MOF-69C	1,4-BDC	$Zn_3(OH)_2(1,4\text{-}BDC)_2 \cdot (DEF)_2$ *P2₁/n*; 17.664, 14.848, 18.129; 90.00, 112.140, 90.00; 4404.5; 6
MOF-70	1,4-BDC	$Pb(1,4\text{-}BDC)(EtOH) \cdot (EtOH)$ *P2/n*; 8.3639, 17.9915, 9.9617; 90.00, 102.687, 90.00; 1462.4; 4
MOF-71	1,4-BDC	$Co(1,4\text{-}BDC)(DMF)$ *Imma*; 19.2301; 7.2387; 8.8482; 90.00, 90.00, 90.00; 1231.7; 16
MOF-72	1,3-BDC	$Cd_3(1,3\text{-}BDC)_4 \cdot (Me_2NH_2)_2$ *C2/c*; 13.686, 18.252, 14.906; 90.00, 101.070, 90.00; 3654.2; 8
MOF-73	1,4-BDC	$Mn_3(1,4\text{-}BDC)_3(DEF)_2$ *C2/c*; 24.7821, 10.5843, 17.4219; 90.00, 129.9320, 90.00; 3504.1; 8
MOF-74	DHBDC	$Zn_2(DHBDC)(H_2O)_2 \cdot (H_2O)_{0.5}(EtOH)_{1.5}$ *R(-3)*; 25.9322, 25.9322, 6.8365; 90.00, 90.00, 120.00; 3981.5; 9
MOF-75	TDC	$Tb(TDC)(NO_3)(DMF)_2$ *P2₁/n*; 10.6926, 10.6727, 15.7533; 90.00, 95.865, 90.00; 1788.3; 4
MOF-76	BTC	$Tb(BTC)(H_2O)_{1.5} \cdot (DMF)$ *P4₃22*; 10.2792, 10.2792, 14.5376; 90.00, 90.00, 90.00; 1536.1; 4
MOF-77	ATC	$Zn_4(ATC)$ *I4₁/a*; 7.2607, 7.2607, 25.4712; 90.00, 90.00, 90.00; 1342.8; 8
MOF-78	HPDC	$Co(HPDC)(H_2O)(DMF)_2$ *C2/c*; 29.6774, 9.6296, 7.9813; 90.00, 97.680, 90.00; 2260.3; 4
MOF-79	HPDC	$Cd_2(HPDC)_2(CHP) \cdot (H_2O)$ *P-1*; 10.1023, 14.4120, 14.9635; 70.590, 72.752, 87.142; 1959.5; 2
MOF-80	PDC	$Tb(PDC)_{1.5}(H_2O)_2(DMF) \cdot (DMF)$ *P-1*; 9.8294, 12.1099, 14.6280; 109.750, 103.613, 100.140; 1529.3; 2

a BPDC = 4,4′-biphenyldicarboxylate; NDC = 2,6-naphthalenedicarboxylate; 1,4-BDC = 1,4-benzenedicarboxylate; 1,3-BDC = 1,3-benzenedicarboxylate; DHBDC = 2,5-dihydroxybenzenedicarboxylate; TDC = 2,5-thiophenedicarboxylate; BTC = 1,3,5-benzenetricarboxylate; ATC = 1,3,5,7-adamantanetetracarboxylate; HPDC = 2,7-tetrahydropyrenedicarboxylate; PDC = 2,7-pyrenedicarboxylate. *b* DEF = diethylformamide; EtOH = ethanol; DMF = dimethylformamide; CHP = 1-cyclohexyl-2-pyrolidinone.

"guest-free" form. Pressures were measured with two MKS Baratron transducers 622A with the range covering 0−10 and 0−1000 Torr (accuracy 0.25%). The adsorbate was added incrementally. A point isotherm was recorded at equilibrium (obtained when no further weight change was observed and the pressure changes were less than 1 mm Torr/min).

The N_2, Ar, and CO_2 adsorbates were of UHP grade. The temperature of each sample was controlled using a refrigerated bath of liquid nitrogen (−195 °C) for N_2 and Ar sorption measurements. All organic solvents were GC grade 99.9%, purchased from Aldrich Chemical Co. and stored over molecular sieves. The nitrogen apparent Langmuir surface area was estimated using the Langmuir equation and assuming monolayer coverage of N_2 using a cross-sectional area of 16.2 $Å^2$/molecule. The pore volume was calculated by extrapolation of the Dubinin−Radushkevich equation, assuming the sorbate is in a liquidlike state and a pore-filling sorption process.[15]

Synthesis of Compounds. $Zn_3(OH)_2(BPDC)_2 \cdot (DEF)_4(H_2O)_2$: MOF-69A. A solid mixture of $Zn(NO_3)_2 \cdot 6H_2O$ (24.6 mg, 0.083 mmol) and 4,4′-biphenyldicarboxylic acid (H_2BPDC) (10 mg, 0.041 mmol) was dissolved in a 20 mL vial containing DEF (12 mL), 30% H_2O_2 (0.40 mL), and CH_3NH_2 (0.20 mL, 70.3 mM in DMF). The mixture was allowed to stand in a capped vial for 7 d at room temperature. Colorless crystals of MOF-69A were collected and air-dried (21 mg, 86.1% yield based on H_2BPDC). This compound is insoluble in common organic solvents. Anal. Calcd for $C_{48}H_{66}N_4O_{16}Zn_3$ = MOF-69A: C, 50.08; H, 5.78; N, 4.87; Zn, 17.04. Found: C, 50.81; H, 5.48; N, 5.16; Zn, 16.13. FT-IR (KBr 4000−400 cm^{-1}): 3415 (br), 3071 (w), 2974 (w), 2935 (w), 2876 (w), 1675 (s), 1642 (s), 1596 (s), 1548 (m), 1404 (s), 1313 (w), 1263 (w), 1218 (w), 1178 (w), 1110 (w), 1005 (w), 942 (w), 845 (w), 823 (w), 801 (w), 774 (s), 702 (w), 686 (w), 645 (w), 584 (w), 468 (w).

$Zn_3(OH)_2(NDC)_2 \cdot (DEF)_4(H_2O)_2$: MOF-69B. A solid mixture of $Zn(NO_3)_2 \cdot 6H_2O$ (24.6 mg, 0.083 mmol) and 2,6-naphthalenedicarboxylic acid (H_2NDC) (8.9 mg, 0.041 mmol) was dissolved in a 20 mL vial containing DEF (12 mL), 30% H_2O_2 (0.40 mL), and CH_3NH_2 (0.20 mL, 70.3 mM in DMF). The mixture was allowed to stand in a capped vial for 7 d at room temperature. Colorless crystals of MOF-69B were collected and air-dried (18 mg, 80.4% yield based on H_2NDC). This compound is insoluble in common organic solvents. Anal. Calcd for $C_{44}H_{62}N_4O_{16}Zn_3$ = MOF-69B: C, 48.08; H, 5.69; N, 5.10; Zn, 17.85. Found: C, 48.28; H, 5.13; N, 5.02; Zn, 17.76. FT-IR (KBr 4000−400 cm^{-1}): 3440 (br), 2977 (w), 2935 (w), 2882 (w), 1645 (s), 1607 (s), 1580 (s), 1502 (w), 1408 (s), 1362 (m), 1264 (w), 1203 (w), 1104 (w), 929 (w), 790 (m), 647 (w), 482 (w).

$Zn_3(OH)_2(1,4\text{-}BDC)_2 \cdot (DEF)_2$: MOF-69C. In a 20 mL vial, a solid mixture of 1,4-benzenedicarboxylic acid (1,4-BDC) (33.0 mg, 0.199 mmol) and $Zn(NO_3)_2 \cdot 6H_2O$ (177 mg, 0.596 mmol) was dissolved in DEF (4.883 mL). Deionized H_2O (0.117 mL) was added to the reaction solution, and the vial was capped and heated for 15 h in a 100 °C isotemp oven. The vial, containing colorless rodlike crystals (67 mg, 89% yield based on H_2BDC), was removed from the oven while hot. The crystals were collected and washed with DEF (3 mL × 3). Anal. Calcd for $C_{26}H_{32}N_2O_{12}Zn_3$ = MOF-69C: C, 41.05; H, 4.24; N, 3.68. Found: C, 40.62; H, 4.29; N, 3.53. FT-IR (KBr 4000−400 cm^{-1}): 3342 (br), 2984 (m), 2940 (w), 2884 (w), 1650 (s), 1584 (s), 1504 (m), 1450 (m), 1407 (s), 1298 (w), 1259 (w), 1213 (w), 1157 (w), 1109 (m), 1019 (m), 915 (w), 826 (s), 751 (s), 647 (w), 599 (m), 527 (m), 435 (m).

$Pb(1,4\text{-}BDC)(C_2H_5OH) \cdot (C_2H_5OH)$: MOF-70. In a 20 mL vial, lead(II) nitrate (60 mg, 0.181 mmol) and 1,4-benzenedicarboxylic acid (H_2BDC) (30 mg, 0.181 mmol) were dissolved in DMF (1 mL) and then diluted with ethanol (9 mL). To this solution was added hydrogen peroxide aqueous solution (30%) (0.1 mL) to give a clear colorless solution. Eight vials of this solution were placed along the perimeter

(15) Gregg, S. J.; Sing, K. S. W. *Adsorption, Surface Area and Porosity*, 2nd ed.; Academic Press: London, U.K., 1982.
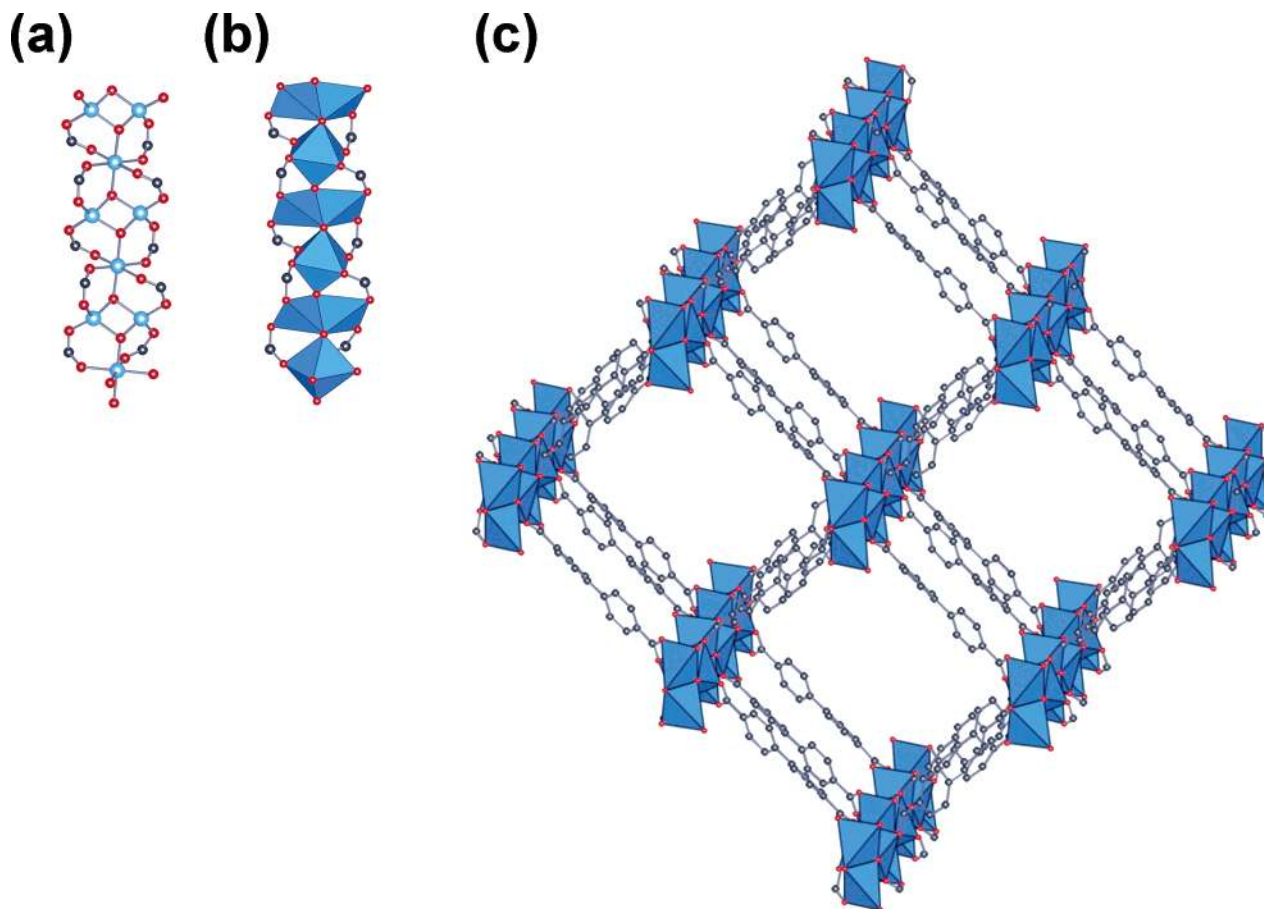
MOF-69A

Figure 4. MOF-69A: ball-and-stick representation of SBU (a); SBU with Zn shown as polyhedra (b); and view of crystalline framework with inorganic SBUs linked together via biphenyl rings of 4,4′-biphenyldicarboxylate (c) (DEF and H_2O guest molecules have been omitted for clarity). All drawing conditions are the same as in Figure 3, with Zn in blue.

of a big container. Triethylamine (0.4 mL) (TEA) was added to DMF (5 mL) and then placed in a vial in the center of the big container. The container was covered, and the TEA solution was allowed to diffuse into the solutions containing $Pb(NO_3)_2$ and H_2BDC. After 1 week, colorless crystals were produced, collected, and washed with ethanol and DMF mixed solution (90% ethanol, 10% DMF). The crystals became opaque upon exposure to air. Anal. Calcd for $C_{12}H_{16}O_6Pb$ = MOF-70: C, 31.10; H, 3.48; N, 0.00. Found: C, 27.60; H, 1.96; N, 0.38. FT-IR (KBr 4000−400 cm^{-1}): 3407 (br), 3058 (w), 2937 (w), 1643 (m), 1525 (s), 1448 (m), 1400 (s), 1360 (s), 1176 (w), 1150 (m), 1131 (w), 1104 (w), 1051 (m), 1025 (sh), 997 (w), 900 (m), 867 (m), 834 (m), 814 (sh), 755 (sh), 708 (w), 688 (w), 558 (m), 511 (sh).

Co(1,4-BDC)(DMF): MOF-71. A solid mixture of $Co(NO_3)_2$·$6H_2O$ (40 mg, 0.137 mmol) and 1,4-benzenedicarboxylic acid (23 mg, 0.137 mmol) was dissolved in DMF (1 mL) and absolute EtOH (0.25 mL). The resulting solution was transferred with a pipet into a Pyrex tube, frozen in a $N_{2(l)}$ bath, evacuated (200 mTorr), and flame-sealed. The sealed reaction tube was heated for 15 h in a 100 °C isotemp oven. The tube, containing pink blocklike crystals and purple hexagonal platelike crystals, was removed from the oven while hot. The mixture of crystals was collected and washed with DMF (3 mL × 3). The two crystalline phases were separated by density (CHBr$_3$/CH$_2$Cl$_2$), and the pink blocklike crystals (17 mg, 84% based on H_2BDC) were characterized. Anal. Calcd for $C_{11}H_{11}NO_5Co$ = MOF-71: C, 44.61; H, 3.74; N, 4.73. Found: C, 43.37; H, 3.45; N, 4.26. FT-IR (KBr 4000−400 cm^{-1}): 3441 (br), 3072 (w), 2946 (w), 2814 (w), 1636 (m), 1586 (m), 1389 (s), 1118 (w), 1017 (w), 820 (w), 747 (m), 671 (w), 538 (w), 430 (w).

Cd$_3$(1,3-BDC)$_4$·(Me$_2$NH$_2$)$_2$: MOF-72. A solid mixture of 1,3-benzenedicarboxylic acid (H$_2$-1,3-BDC) (24 mg, 0.145 mmol) and Cd-(NO$_3$)$_2$·$4H_2O$ (22.20 mg, 0.072 mmol) was dissolved in DMF (1 mL). The resulting solution was transferred into a Pyrex tube by pipet. To the solution was added a CH_3NH_2/H_2O/DMF solution (0.1 mL) prepared by diluting 40% aqueous CH_3NH_2 (1 mL) with DMF (50 mL). The tube was frozen in a $N_{2(l)}$ bath, evacuated (200 mTorr), flame-sealed, and heated to 140 °C at a rate if 5 °C/min for 50 h and then cooled to room temperature at a rate of 2 °C/min. Colorless rod-shaped crystals of the product were formed, collected, washed with DMF (3 mL × 3), and air-dried (24 mg, 31% based on H$_2$-1,3-BDC). Anal. Calcd for $C_{36}H_{32}N_2O_{16}Cd_3$ = MOF-72: C, 39.82; H, 2.97; N, 2.58. Found: C, 39.47; H, 2.94; N, 2.72. FT-IR (KBr 4000−400 cm^{-1}): 3450 (br), 3068 (w), 2934 (w), 1659 (s), 1608 (s), 1561 (m), 1480 (w), 1445 (w), 1388 (s), 1162 (w), 1021 (w), 832 (w), 747 (m), 725 (m), 661 (w).

Mn$_3$(BDC)$_3$(DEF)$_2$: MOF-73. A solid mixture of 1,4-benzenedicarboxylic acid (H$_2$BDC) (17 mg, 0.102 mmol) and Mn(ClO$_4$)$_2$·$6H_2O$ (108 mg, 0.298 mmol) was dissolved in DEF (2.0 mL). This solution was decanted into a Pyrex tube which was then frozen in a $N_{2(l)}$ bath, evacuated (200 mTorr), flame-sealed, and heated for 48 h in a 100 °C isotemp oven. The tube, containing colorless rhombus-shaped block crystals, was removed from the oven while hot. The crystals were washed with DEF (3 mL × 3) and air-dried to yield pure product (7 mg, 21.4% based on H$_2$BDC). Anal. Calcd for $C_{34}H_{34}NO_{14}Mn_3$ = MOF-73: C, 47.52; H, 3.99; N, 3.24. Found: C, 45.67; H, 3.76; N, 3.24. FT-IR (KBr 4000−400 cm^{-1}): 3440 (br), 3131 (w), 3091 (w), 3056
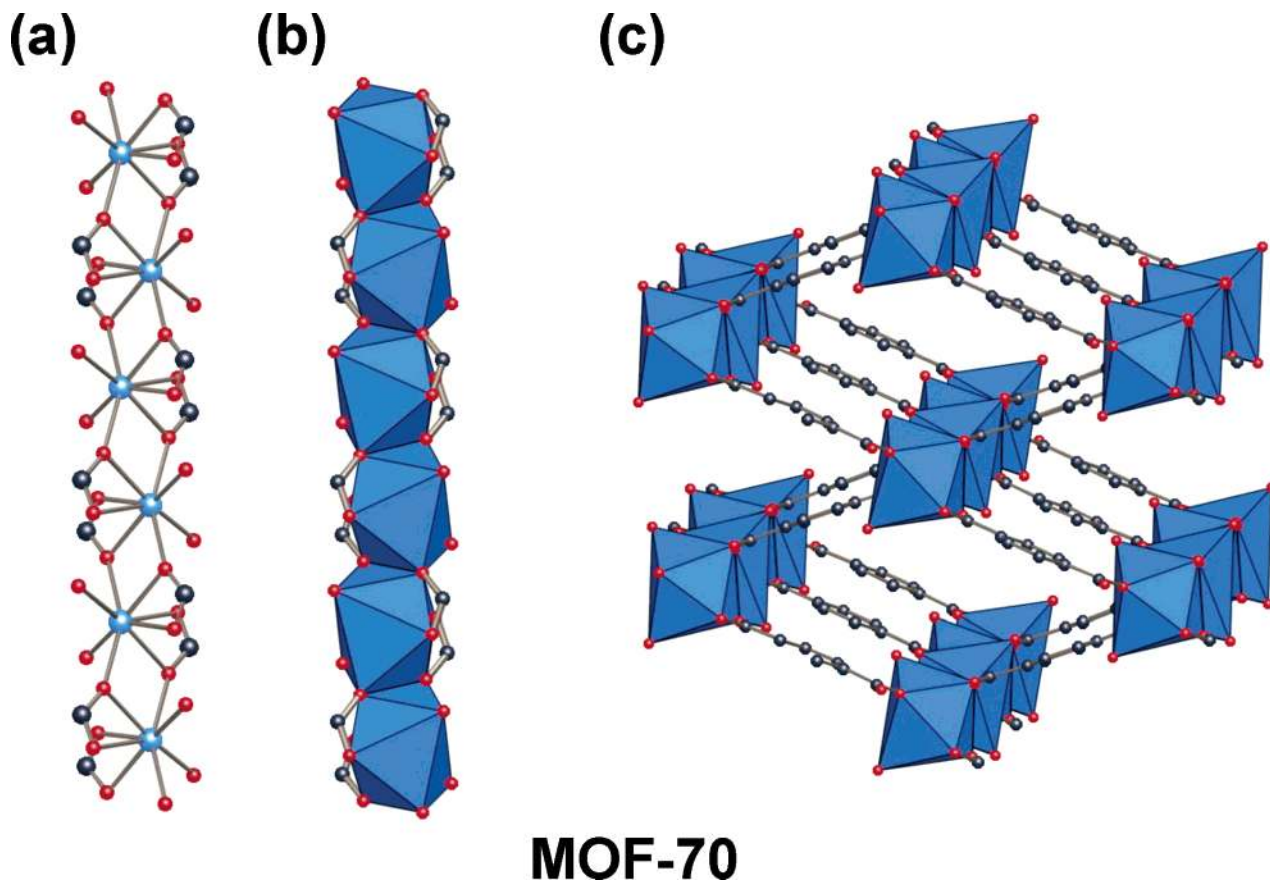
MOF-70

Figure 5. MOF-70: ball-and-stick representation of SBU (a); SBU with Pb shown as polyhedra (b); and view of crystalline framework with inorganic SBUs linked together via the benzene ring of 1,4-benzenedicarboxylate (c) (EtOH guest molecules have been omitted for clarity). All drawing conditions are the same as in Figure 3, with Pb in blue.

(w), 2976 (w), 2940 (w), 1652 (s), 1574 (m), 1509 (m), 1395 (s), 1265 (w), 1212 (w), 1124 (w), 1019 (w), 889 (w), 826 (m), 750 (s), 662 (w), 519 (m).

$Zn_2(DHBDC)(DMF)_2\cdot(H_2O)_2$: MOF-74. A solid mixture of 2,5-dihydroxy-1,4-benzenedicarboxylic acid (H_2-DHBDC) (0.019 g, 0.096 mmol) and zinc nitrate tetrahydrate, $Zn(NO_3)_2\cdot4(H_2O)$ (0.053 mg, 0.203 mmol), was dissolved in DMF (2.0 mL), 2-propanol (0.1 mL), and water (0.1 mL) and placed in a Pyrex tube which was then frozen in a $N_{2(l)}$ bath, evacuated (200 mTorr), flame-sealed, and heated to 105 °C at a rate of 2.0 °C/min for 20 h and then cooled to room temperature at a rate of 2.0 °C/min. Yellow needle crystals were produced which were dried in air after washing with DMF and ethanol (26 mg, yield 51% based on H_2-DHBDC). Anal. Calcd for $C_{14}H_{20}N_2O_{10}Zn_2$ = MOF-74: C, 33.16; H, 3.98; N, 5.52. Found: C, 32.93; H, 3.59; N, 5.33. FT-IR (KBr, 4000−400 cm^{-1}): 3440 (br), 2931 (w), 2818 (w), 1662 (s), 1555 (s), 1459 (m), 1408 (s), 1367 (w), 1245 (m), 1204 (s), 1112 (w), 913 (w), 888 (m), 812 (s), 674 (w), 633 (w), 587 (w), 480 (w).

$Tb(TDC)(NO_3)(DMF)_2$: MOF-75. A solid mixture of $Tb(NO_3)_3\cdot5H_2O$ (109 mg, 0.251 mmol) and 2,5-thiophenedicarboxylic acid (H_2-TDC) (11.5 mg, 0.067 mmol) was dissolved in DMF (1 mL). 2-Propanol (1.5 mL) was added to the DMF solution. The resulting solution was transferred with a pipet into a Pyrex tube, frozen in a $N_{2(l)}$ bath, evacuated (200 mTorr), and flame-sealed. The sealed reaction tube was heated to 85 °C at a rate of 2 °C/min for 15 h and then cooled to room temperature at a rate of 2 °C/min to yield colorless polyhedral crystals (30.6 mg, 84% based on H_2TDC). Anal. Calcd for $C_{12}H_{16}N_3O_9STb$ = MOF-75: C, 26.83; H, 3.00; N, 7.82. Found: C, 26.63; H, 2.87; N, 7.68. FT-IR (KBr 4000−400 cm^{-1}): 3455 (br), 3099 (w), 2941 (w), 1692 (s), 1657 (s), 1617 (s), 1586 (s), 1525 (m), 1459 (m), 1372 (s), 1316 (m), 1112 (w), 1041 (w), 797 (w), 776 (m), 685 (m), 466 (w).

$Tb(BTC)(H_2O)_{1.5}\cdot(DMF)$: MOF-76. To a solvothermal vessel were added H_3BTC (0.020 g, 0. 10 mmol), $Tb(NO_3)_3\cdot5H_2O$ (0.120 g, 0.28 mmol), DMF (4 mL), ethanol (4 mL), and H_2O (3.2 mL), respectively. The vessel was sealed and heated to 80 °C at a rate of 2 °C/min for 24 h and then cooled to room temperature at a rate of 1 °C/min. Needlelike colorless crystals of the product were formed and collected by filtration (35 mg, 78% yield based on H_3BTC). The product is stable in air and insoluble in water and common organic solvents such as ethanol, acetonitrile, acetone, chloroform, and DMF. Anal. Calcd for $C_{12}H_{13}$-$NO_{8.5}Tb$ = MOF-76: C, 30.92; H, 2.81; N, 3.00. Found: C, 31.03; H, 2.74; N, 2.93. FT-IR (KBr, 4000−400 cm^{-1}): 3434 (br), 2934 (w), 1670 (s), 1631 (s), 1618 (s), 1578 (m), 1545 (m), 1446 (s), 1387 (s), 1111 (w), 946 (w), 775 (m), 709 (m), 571 (w), 459 (w).

$Zn_2(ATC)$: MOF-77. To a solvothermal vessel were added adamantane tetracarboxylic acid (H_4ATC) (0.048 g, 0.15 mmol), $Zn(NO_3)_2\cdot6H_2O$ (0.140 g, 0.47 mmol), and H_2O (4 mL), respectively. The vessel was sealed and heated to 185 °C at a rate of 5 °C/min for 40 h and then cooled to room temperature at a rate of 2 °C/min. Tetragonal colorless crystals of the product were formed and collected by filtration, yielding 0.058 g (86% yield based on H_4ATC). The product is stable in air and insoluble in water and common organic solvents such as ethanol, acetonitrile, acetone, chloroform, and DMF. Anal. Calcd for $C_{14}H_{12}O_8Zn_2$ = MOF-77: C, 38.30; H, 2.76. Found: C, 38.41; H, 2.82. FT-IR (KBr, 4000−400 cm^{-1}): 3441 (br), 2954 (w), 2869 (w), 1618 (s), 1532 (s), 1420 (s), 1210 (m), 723 (m), 591 (w), 486 (w).

$Co(HPDC)(H_2O)(DMF)_2$: MOF-78. H_2HPDC (0.018 g, 0.06 mmol) was dissolved in DMF (7.0 mL) and EtOH (2.0 mL). To deprotonate the acid, 0.10 mL of a triethylamine/ethanol solution (5.0% v/v) was added to the organic solution and sonicated (1 min). $Co(NO_3)_2\cdot6H_2O$ (0.060 g, 0.21 mmol) was dissolved in water (1.0 mL), which
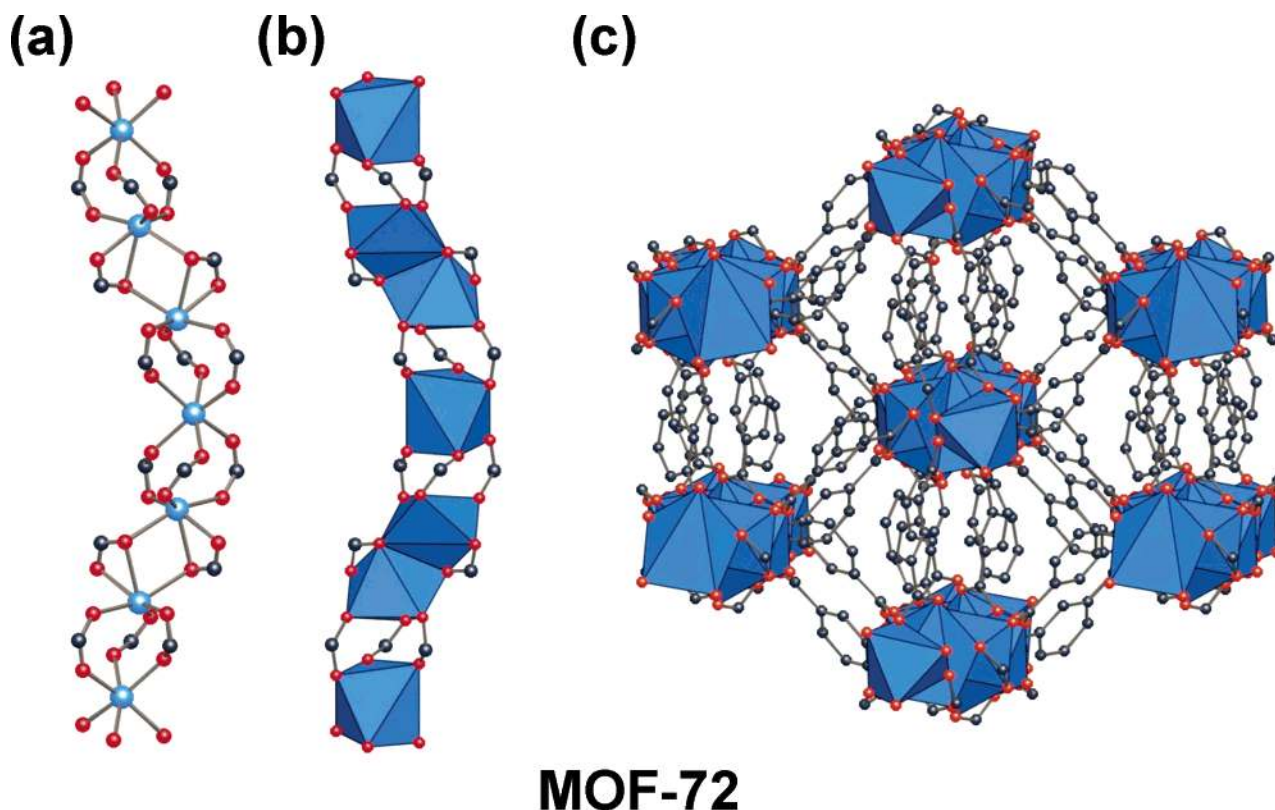
MOF-72

Figure 6. MOF-72: ball-and-stick representation of SBU (a); SBU with Cd shown as polyhedra (b); and view of crystalline framework with inorganic SBUs linked together via the benzene ring of 1,3-benzenedicarboxylate (c) (Me$_2$NH$_2$ guest cations have been omitted for clarity). All drawing conditions are the same as in Figure 3, with Cd in blue.

was poured into the mixed solution, and the whole solution was mixed using a sonicator (1 min). The resulting clear pink solution was placed in a solvothermal vessel which was sealed and heated to 85 °C for 24 h and cooled to room temperature at a rate of 1.0 °C/min. Rectangular pink crystals were produced which were dried in air after washing with DMF and acetone (0.024 g, 77% based on one acid). Anal. Calcd for C$_{24}$H$_{28}$N$_2$O$_7$Co = Co(HPDC)(H$_2$O)(DMF)$_2$: C, 55.93; H, 5.48; N, 5.43. Found: C, 55.45; H, 5.54; N, 3.76. FT-IR (KBr, 4000−400 cm^{-1}): 3434 (br), 2934 (w), 2888 (w), 2835 (w), 2079 (br), 1664 (s), 1578 (m), 1539 (s), 1466 (w), 1433 (w), 1394 (vs), 1354 (s), 1300 (w), 1242 (m), 1117 (m), 1058 (m), 1006 (w), 929 (m), 802 (m), 749 (s), 595 (br), 459 (w).

Cd$_2$(HPDC)$_2$(CHP)·(H$_2$O): MOF-79. H$_2$HPDC (0.018 g, 0.061 mmol) and Cd(NO$_3$)$_2$·4H$_2$O (0.055 g, 0.18 mmol) were suspended in water (2.0 mL), CH$_3$OH (3.0 mL), and 1-cylcohexyl-2-pyrrolidinone (CHP) (3.0 mL), and the resulting mixture was dispersed by sonication (1 min). The heterogeneous mixture was placed in a solvothermal vessel which was sealed and heated to 130 °C at a rate of 2.0 °C/min for 20 h and then cooled to room temperature at a rate of 2.0 °C/min. Rectangular pale yellow crystals were produced which were dried in air after washing with DMF and ethanol (0.026 g, yield 52% based H$_2$TPDC). Anal. Calcd for C$_{46}$H$_{43}$NO$_{10}$Cd$_2$ = MOF-79: C, 55.55; H, 4.35; N, 1.41. Found: C, 55.62; H, 4.25; N, 1.43. FT-IR (KBr, 4000−400 cm^{-1}): 3408 (br), 2932 (m), 2857 (w), 2867 (w), 1634 (s), 1606 (w), 1586 (w), 1571 (w), 1503 (w), 1467 (w), 1427 (w), 1396 (vs), 1380 (vs), 1348 (vs), 1300 (w), 1241 (w), 1129 (w), 1034 (w), 907 (br), 819 (w), 795 (m), 775 (m), 764 (m), 696 (w), 577 (w), 549 (w).

Tb(PDC)$_{1.5}$(H$_2$O)$_2$(DMF)·(DMF): MOF-80. H$_2$PDC (0.010 g, 0.034 mmol) and Tb(NO$_3$)$_3$·5H$_2$O (0.056 g, 0.129 mmol) were suspended in water (2.0 mL), ethanol (4.0 mL), and DMF (4.0 mL), and the resulting mixture was dispersed by sonication (1 min). The heterogeneous mixture was placed in a solvothermal vessel which was sealed and heated at a rate of 2.0 °C/min to 80 °C for 24 h and then cooled to room temperature at a rate of 1.0 °C/min. Rectangular pale

yellow crystals were produced which were dried in air after washing with DMF and ethanol (0.013 g, 73% based on one acid). Anal. Calcd for C$_{33}$H$_{30}$N$_2$O$_{10}$Tb = MOF-80: C, 51.24; H, 3.91; N, 3.62. Found: C, 51.13; H, 3.78; N, 3.21. FT-IR (KBr, 4000−400 cm^{-1}): 3480 (br), 3059 (w), 2934 (w), 1670 (s), 1651 (w), 1617 (w), 1600 (m), 1563 (s), 1558 (s), 1460 (s), 1400 (vs), 1314 (w), 1262 (s), 1111 (m), 1065 (w), 913 (s), 820 (s), 782 (m), 736 (s), 709 (m), 676 (w), 599 (br).

Porosity Measurements. Mn$_3$(BDC)$_3$(DEF)$_2$: MOF-73. A sample of MOF-73 (15.153 mg) was heated under a N$_2$ atmosphere from 25 to 600 °C at a rate of 1 °C/min in a gravimetric analyzer. A 22.9% weight loss was observed from 115 to 350 °C, which corresponds to the loss of one DEF molecule per formula unit (calcd: 23.5%). The sample begins decomposing at 400 °C. Sorption isotherms for MOF-73 were completed for both N$_2$ and CHCl$_3$ by measuring the increase in weight at equilibrium as a function of relative pressures of the sorbate. The sample was subjected to heating (275 °C/15 h) at pressures below 1 × 10^{-5} Torr to remove the guests and produce the evacuated form. The sorption isotherms for N$_2$ and CHCl$_3$ are discussed in the Results and Discussion section. The apparent surface area and the pore volume were estimated to be 181 m^2/g and 0.061 cm^3/g, respectively.

Zn$_2$(DHBDC)(DMF)$_2$·(H$_2$O)$_2$: MOF-74. The as-synthesized crystals (100 mg) were placed in 10 mL of water in a 20 mL vial for 30 min. The water was decanted, and an additional 10 mL of water was added to the vial, which was then allowed to stand at room temperature for 1 h. The water was decanted again, and the crystals were washed with ethanol (5 × 10 mL). The crystals were finally dried in air. The elemental microanalysis data indicated that there was essentially no DMF in the sample with the nitrogen content less than 0.1% (Anal. Calcd for C$_{11}$H$_{16}$N$_0$O$_{10}$Zn$_2$ = Zn$_2$(DHBDC)(H$_2$O)$_2$·(H$_2$O)$_{0.5}$(C$_2$H$_5$-OH)$_{1.5}$: C, 30.09; H, 3.67; N, 0.00. Found: C, 30.03; H, 4.01; N, <0.10). FT-IR data also showed the absence of the carbonyl peak of DMF (1662 cm^{-1}), which was strongly observed in the as-synthesized samples. On the other hand, the ν_{OH} peak became more intense. However, the observed XRPD showed the same peak pattern as those
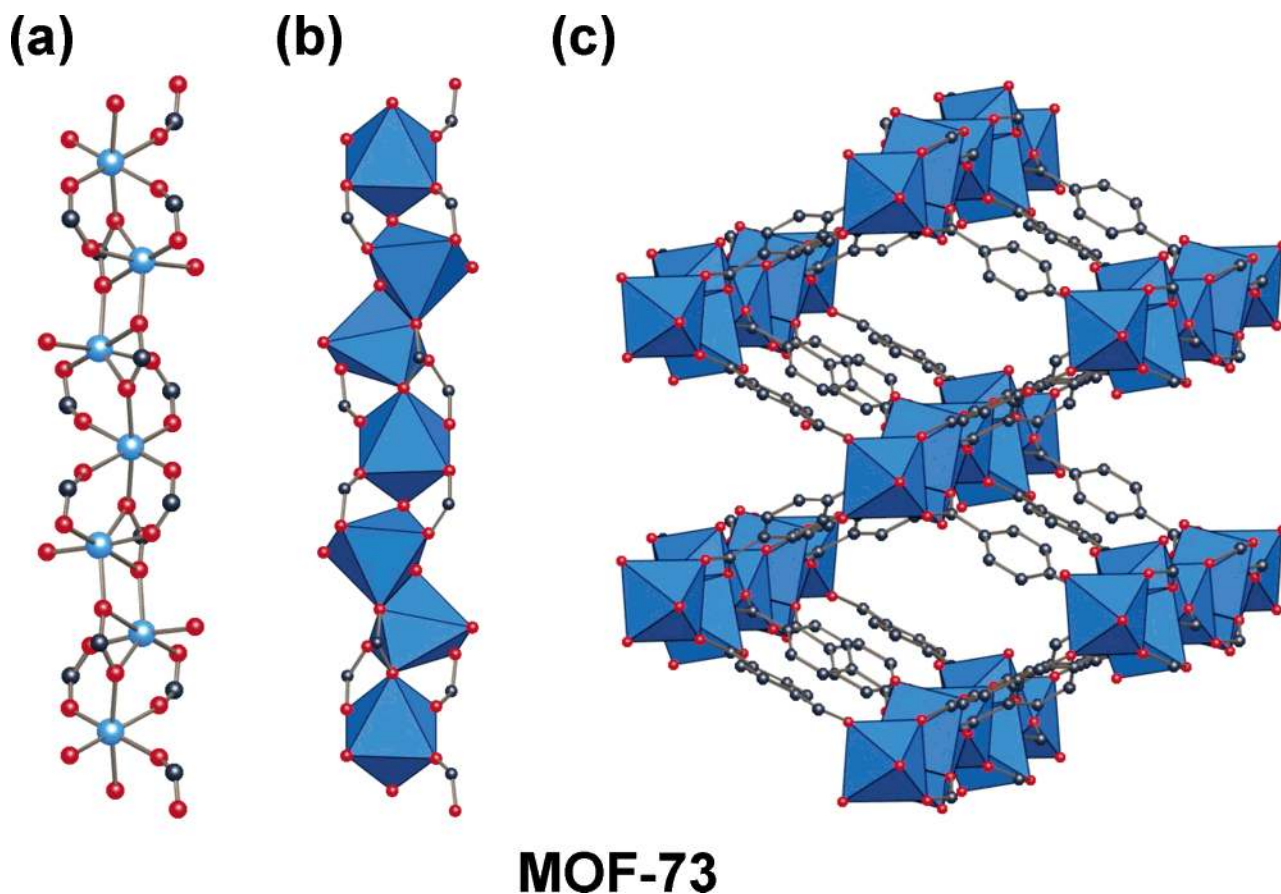
MOF-73

Figure 7. MOF-73: ball-and-stick representation of SBU (a); SBU with Mn shown as polyhedra (b); and view of crystalline framework with inorganic SBUs linked together via the benzene ring of 1,4-benzenedicarboxylate (c) (DEF guest molecules have been omitted for clarity). All drawing conditions are the same as in Figure 3, with Mn in blue.

of the as-synthesized material, which indicates the maintenance of the original frameworks. FT-IR (KBr, 4000−400 cm^{-1}): 3409 (br), 2981 (w), 1555 (s), 1459 (m), 1408 (s), 1245 (m), 1200 (s), 1122 (w), 1087 (w), 1046 (w), 888 (m), 816 (s), 582 (w).

TGA was performed on a sample of this material (14.588 mg). When heated from 20 to 600 °C at 2.0 °C/min, two separate weight-loss steps were observed: (a) 21.0% near 100 °C is attributed to the removal of 1.5 ethanol and 0.5 H_2O molecules per formula unit (calcd. 17.8%), and (b) 8.1% between 125 and 300 °C due to the removal of two coordinated H_2O (calcd. 8.2%). The sample does not show additional weight loss up to 400 °C.

The water-exchanged sample (65.95 mg) was loaded in the sorption apparatus, evacuated to 10^{-4} Torr, and heated to 220 °C for 16 h. Weight loss behavior similar to that observed by TGA was observed, and the final weight converged to 48.94 mg. Nitrogen sorption was performed at 78 K, which resulted in reversible nitrogen uptake and release with a Type I isotherm behavior (see Results and Discussion section). The Langmuir surface area was estimated to be 245 m^2/g.

After the sorption experiment, the sample was heated to 320 °C under vacuum, and the temperature was maintained for 2 h before cooling to room temperature. The XRPD spectrum of the sample showed the same pattern as both the as-synthesized and the water-treated materials.

Tb(BTC)(H$_2$O)$_{1.5}$·(DMF): MOF-76. MOF-76 (54.90 mg) was evacuated at room temperature for 36 h, and the weight was found to be 54.60 mg. Upon heating this sample to 120 °C for 9 h, a weight loss of 15.85% was observed, corresponding to the loss of one DMF molecule per formula unit. N_2 and Ar sorption isotherms are fully reversible and of Type I behavior, characteristic of microporous materials. A similar reversible uptake behavior for organic solvents such as methylene chloride, benzene, and cyclohexane was observed.

Results and Discussion

Metal−Organic Frameworks with Packing of [M$_x$(CO$_2$)$_y$]$_\infty$ Rods.

In this section, we present the structures of MOF-69−80 in the context of their underlying rod packing and their nets. All of the structures are 3-D periodic frameworks and all of the rods are composed of M−O−C units in which the carboxylate links are coordinated to the metal centers in at least one of the following modes:

Modes A, A' and A"   Modes B and B'   Mode C
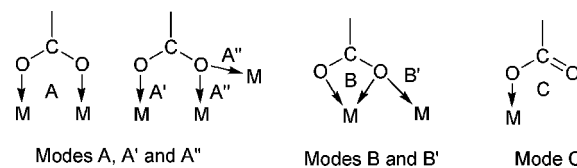
Parallel Packing of Ladder-like Rods: MOF-69A−C. A preliminary account of the synthesis and structure of MOF-69A and B has already appeared;[3] however, we briefly discuss these compounds here, along with MOF-69C, to highlight their relevance to the principles of using rods as building units. The MOF-69A−C compounds have the same underlying topology (isoreticular) as shown in Figure 4. They differ in the nature of the organic link (BPDC for MOF-69A, NDC for MOF-69B, and BDC for MOF-69C) joining the Zn−O−C units. Within these units, there are tetrahedral and octahedral Zn(II) centers, respectively, bound to 4 and 2 carboxylate groups (Figure 4a,b). These groups are coordinated to the Zn by mode A with a μ-3
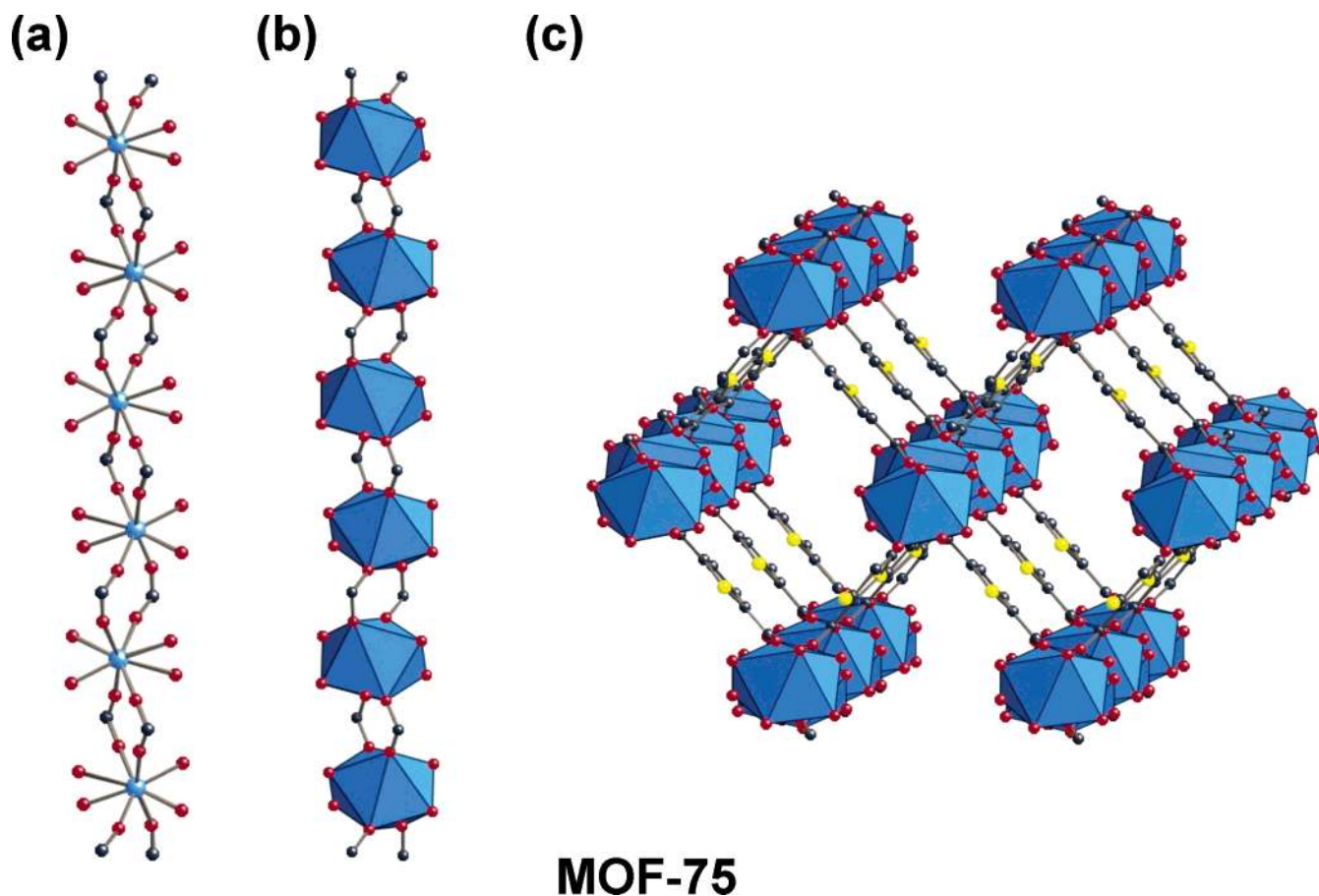
MOF-75

Figure 8. MOF-75: ball-and-stick representation of SBU (a); SBU with Tb shown as polyhedra (b); and view of crystalline framework with inorganic SBUs linked together via the thiophene ring of 2,5-thiophenedicarboxylate (c) (DMF guest molecules and NO_3^- ions have been omitted for clarity). All drawing conditions are the same as in Figure 3, with Tb in blue.

hydroxide ion bridging three Zn centers. The infinite Zn—O—C rods are stacked in parallel and connected in the [110] directions by the respective organic links to give 1-D rhombic channels of 12.2 Å along an edge and 16.6 Å along the diagonal (MOF-69A) into which four DEF and two water molecules per formula unit reside as guests (for MOF-69A and B; two DEF molecules in MOF-69C) (Figure 4c). For MOF-69A—C, two DEF molecules were found hydrogen bonded to the μ-3 hydroxyl groups (O···H···OC = 2.81 Å for MOF-69A), while the remaining 2 DEF and 2 water guests are disordered in the pores (MOF69A and B only).

To derive the net of this structure, it is instructive to connect all carboxylate C atoms in the same way as shown in Figure 3c. This gives a tetrahedral net with the C atoms at the vertices. The Zn—O—C rods are ladders, to which the organic links represent the lines that connect the rods together to give the **sra** net topology (Figure 2).

MOF-70. The Pb—O—C rods in this structure are constructed from 8-coordinated Pb(II) centers, where each is bonded to carboxyl groups of four BDC linkers (Figure 5). All carboxyl groups bind in modes B and B′. This connectivity pattern is repeated infinitely to create Pb—O—C rods along the *a* direction and to give edge shared PbO_8 bisdisphenoids. The rods are linked by the benzene rings of BDC, which connect each rod to four neighboring rods in the *c* and *b* directions, generating 13.1 × 5.4 Å^2 1-D rhombic channels in the *a* direction.

Connecting the carboxylate C atoms gives a tetrahedral net that is again that of **sra** (Figure 2).

MOF-71. The structure of the Co—O—C rods are composed of 6-coordinated Co(II) centers having four bridging carboxyl groups using mode A in addition to a doubly bridging oxygen bound DMF ligand. This connectivity pattern is repeated infinitely in the *b* direction, generating linear Co—O—C rods that are zigzag ladders of corner-linked CoO_6 octahedra. Each rod is linked to four neighboring rods by the benzene ring of the BDC units, generating 13.4 × 4.3 Å^2 channels in the *b* direction. The structure is identical to that of MIL-47 and is illustrated in Figure 3a—c; the net of the structure is **sra** (Figure 2).

MOF-72. This structure is constructed from Cd—O—C rods composed of a series of alternating six-coordinated Cd(II) centers (Figure 6). The first is coordinated to six different carboxyl groups in mode A. The second is coordinated to five different carboxyl groups: three in mode A, one in mode B, and one in mode B′. This leads to infinite Cd—O—C rods that run along [10-1]. The rods consist of pairs of edge-sharing CdO_6 polyhedra alternating with isolated CdO_6 polyhedra and are connected to six neighboring rods by the benzene rings of the 1,3-BDC links, resulting in parallel packing of **hex** type (Figure 1 and Table 1). This arrangement leaves open space in the framework for dimethylammonium guests.

MOF-73. The Mn—O—C rods in this compound are constructed from a pair of linked 6-coordinated Mn(II) centers
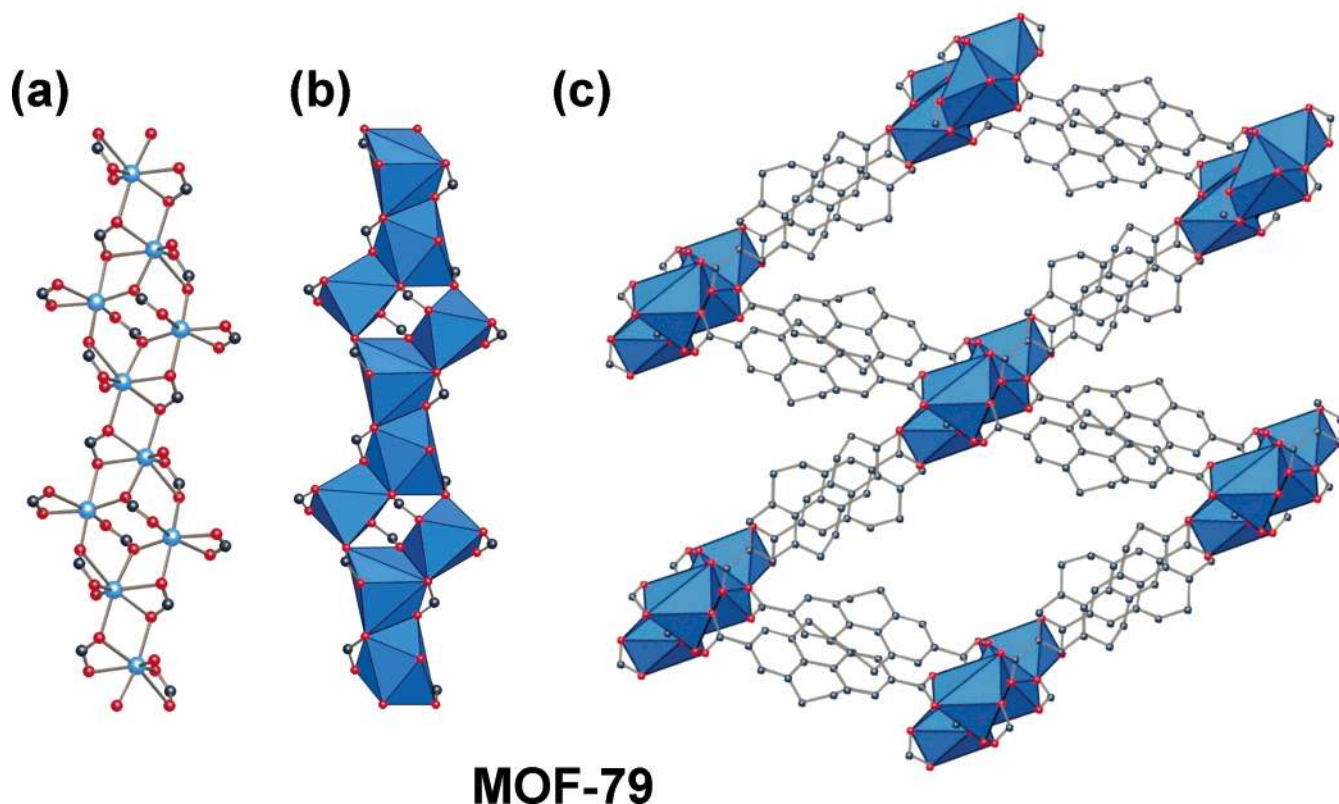
Figure 9. MOF-79: ball-and-stick representation of SBU (a); SBU with Cd shown as polyhedra (b); and view of crystalline framework with inorganic SBUs linked together via the tetrahydropyrene ring of tetrahydropyrenedicarboxylate (c) (CHP guest molecules have been omitted for clarity). All drawing conditions are the same as in Figure 3, with Cd in blue.

(Figure 7). Here, one of the Mn centers has four carboxyl group with two of these bound as in mode A, and one as in mode B, while the remaining one as mode B′. A terminal DEF ligand is also bound to each of these Mn centers. The adjacent Mn center has six carboxyl groups with four bound as in mode A, and two as in mode B′. Each rod is corner-linked and edge-linked MnO_6 polyhedra. The benzene units of the BDC units connect each rod to four neighboring rods, resulting in a **pcu** (Table 1, Figure 1) arrangement with rhombic channels having 11.2×5.9 Å^2 dimensions in which DEF molecules reside as coordinated guests.

MOF-75. In this structure, Tb−O−C rods are composed of 8-coordinated Tb(III) that are bound by four carboxyl groups, one bidentate nitrate ligand, and two DEF terminal ligands (Figure 8). The carboxyl groups are all coordinated according to mode A. This connectivity pattern is repeated infinitely to produce Tb−O−C rods in the *a* crystallographic direction. The rods are linked TbO_8 bisphenoids with the carboxyl carbon atoms forming a twisted ladder that are linked in the *b* and *c* directions by the thiophene units of the TDC links, generating **pcu** type rod packing (Table 1, Figure 1) and rhombic channels in the *a* direction measuring 9.7×6.7 Å^2. The net of the structure is **irl**, the simplest net for linking twisted ladders (Figure 2).

MOF-78. In this structure, the Co−O−C rods are built from 6-coordinated Co(II) centers, to each of which two carboxyl groups, two terminal DMF ligands, and two doubly bridging water ligands are bound. The carboxyl groups are bound in a monodentate fashion according to mode C so they do not fit into our scheme of counting O atoms in the same way as the

other rods of this paper. The HPDC link each rod in the *a* and *b* directions to four neighboring rods, resulting in rhombic channels measuring 23.8×6.7 Å^2 running along the *c* direction. The structure can be simplified by connecting the carboxylate carbon atoms to give a tetrahedral net with the carboxylate carbon atoms at the vertices in the same way as for MOF-71 (cf., Figure 3), thus resulting in the same net (**sra**).

MOF-79. The Cd−O−C rods are built from 6- and 7-coordinated Cd(II) centers and are rather more complex than the other rods described here (Figure 9). Four carboxyl groups and a terminal CHP ligand are bound to the first with two carboxyl groups coordinating as in mode B, one as in A″, and the remaining one as in B′. The other metal center is coordinated by five carboxyl groups with two as in B′, one as A′, one as A″, and the remaining one as in B. These rods are linked by the HPDC link to four other rods to give **pcu** type rod packing (Table 1, Figure 1).

MOF-80. The rods here are composed of chains of 8-coordinated Tb(III) forming square antiprisms (Figure 10). Each Tb is bound by five carboxyl groups, one terminal DMF, and two terminal water ligands. Four of the carboxyl groups are bound according to mode A, and one is bound according to mode C. The rods are linked together along the [011] plane by the PDC connectors to give rod packing of **pcu** type (Table 1, Figure 1) and channels of 19.3×5.8 Å^2 channels running in the *c* direction.

Helical Rods: MOF-74. This structure (Figure 11) is based on coordinated carboxyl and hydroxy groups. Helical Zn−O−C rods of composition $[O_2Zn_2](CO_2)_2$ are constructed from 6-coordinated Zn(II) centers, where each Zn has three carboxyl
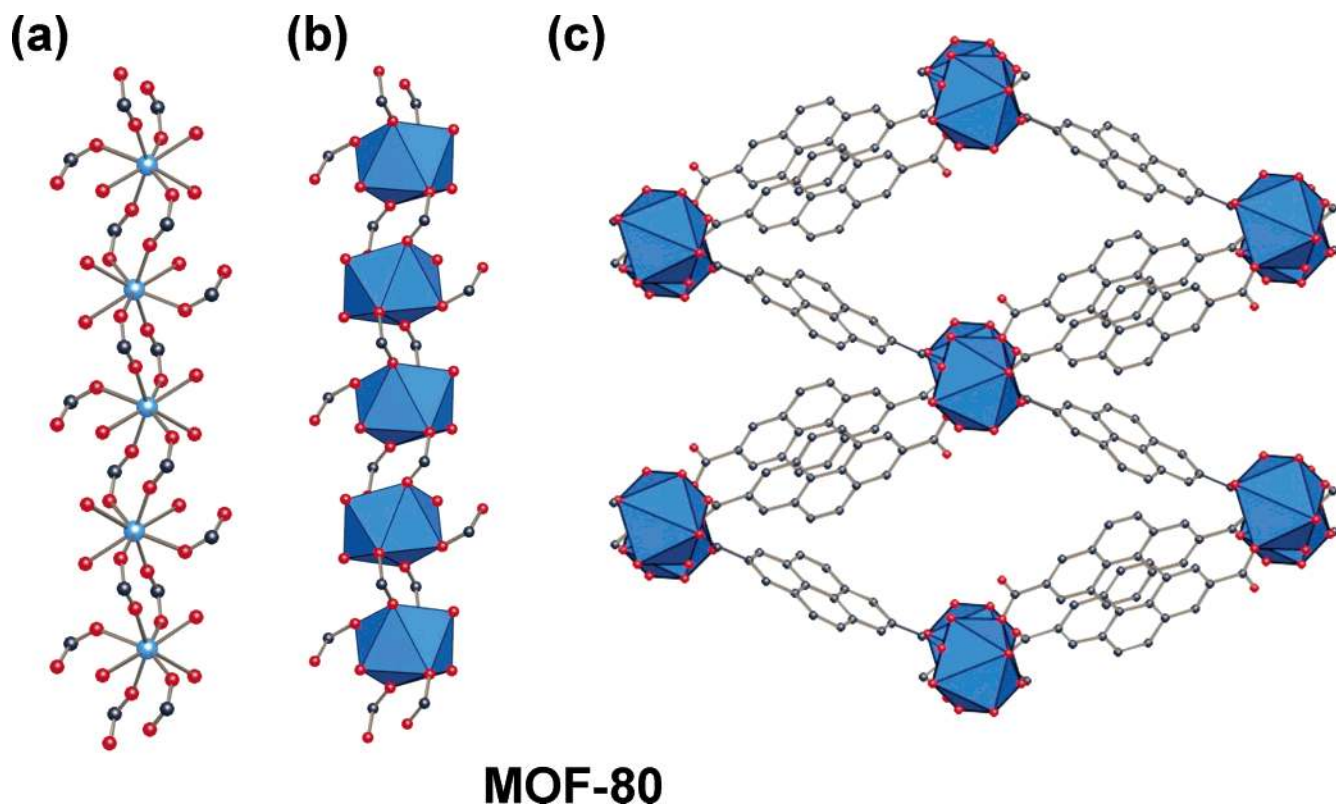
MOF-80

Figure 10. MOF-80: ball-and-stick representation of SBU (a); SBU with Tb shown as polyhedra (b); and view of crystalline framework with inorganic SBUs linked together via the pyrene ring of pyrenedicarboxylate (c) (DMF guest molecules have been omitted for clarity). All drawing conditions are the same as in Figure 3, with Tb in blue.
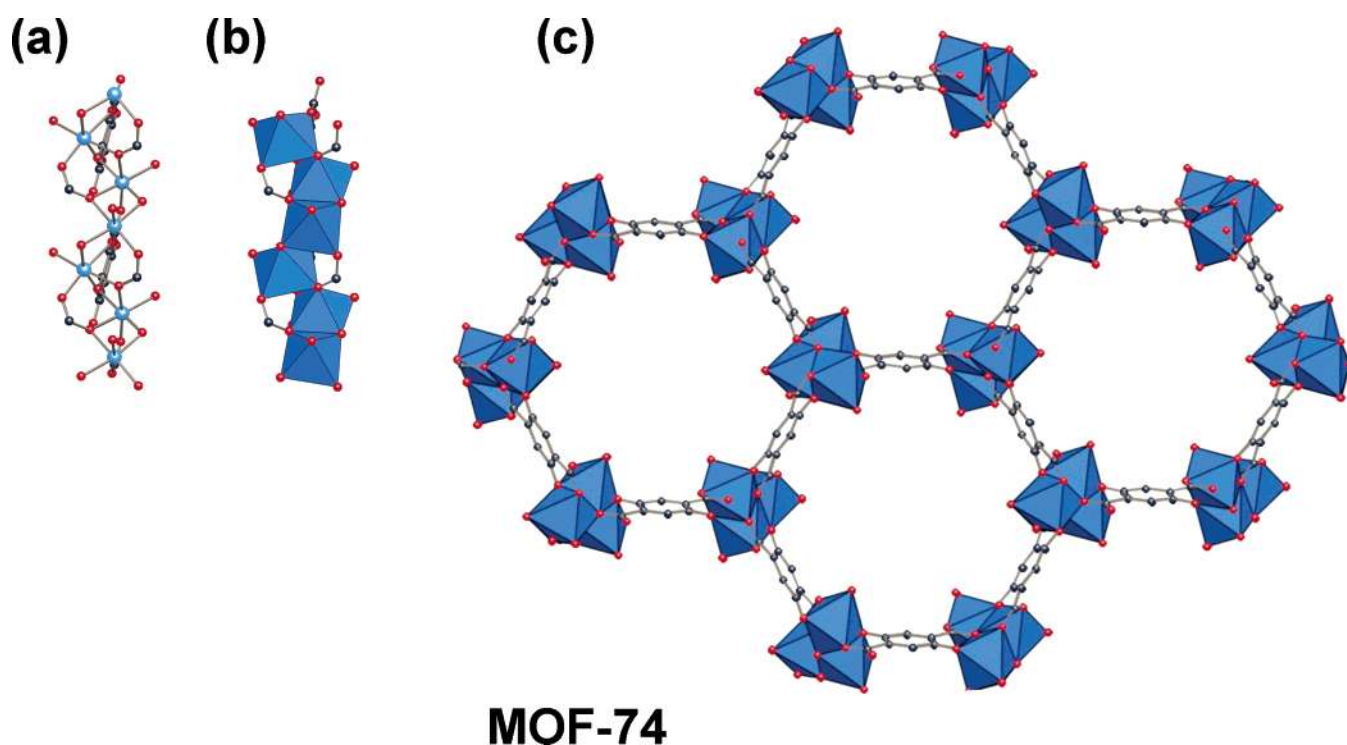

MOF-74

Figure 11. MOF-74: ball-and-stick representation of SBU (a); SBU with Zn shown as polyhedra (b); and view of crystalline framework with inorganic SBUs linked together via the benzene ring of 2,5-dihydroxybenzene-1,4-dicarboxylate (c) (DMF and H_2O guest molecules have been omitted for clarity). All drawing conditions are the same as in Figure 3, with Zn in blue.

groups: one bound as in mode A and the remaining two as in A′. In addition, two hydroxy groups are bound as doubly bridging. The remaining coordination site has a terminal DMF ligand. The rods consist of edge-sharing ZnO_6 octahedra

alternately opposite and next-neighbor to form either a 3_1 or a 3_2 helix. The rods are linked by the benzene units of the DHBDC to produce **bnn** parallel rod packing (Table 1, Figure 1) and one-dimensional channels of dimensions 10.3×5.5 $Å^2$ in which

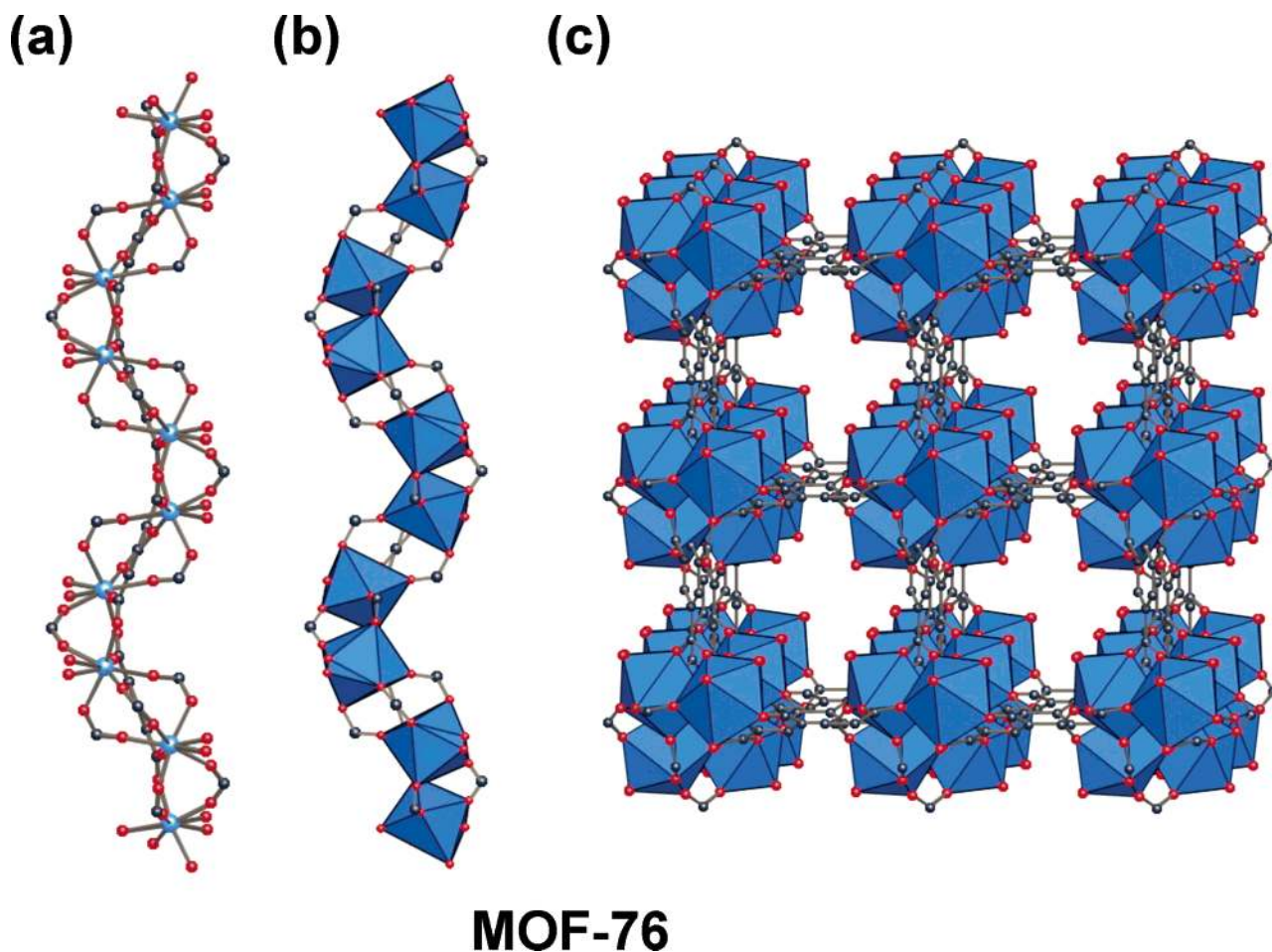# (a)   (b)   (c)

MOF-76

Figure 12. MOF-76: ball-and-stick representation of SBU (a); SBU with Tb shown as polyhedra (b); and view of crystalline framework with inorganic SBUs linked together via the benzene ring of 1,3,5-benzenetricarboxylate (c) (DMF and H_2O guest molecules have been omitted for clarity). All drawing conditions are the same as in Figure 3, with Tb in blue.

terminal DMF molecules protrude and water guests reside. Considering just the carboxylate C atoms as points of extension, they form 3_1 and 3_2 helices that are linked as in net **etb** (Figure 2).

MOF-76. The Tb−O−C units are constructed from 7-coordinated Tb(III) centers (Figure 12). Six carboxyl groups as in mode A and a terminal water ligand bind each Tb. Each rod is connected to four neighboring rods through the benzene ring of the BTC link. The rods pack in a tetragonal fashion, resulting in 6.6×6.6 Å^2 square channels in the *c* direction, which are filled with DMF molecules. Note, however, that the rods themselves are on 4_1 helices, but, because of the tritopic nature of the organic SBU, result in a rather complicated overall topology.

Tetragonal Layer Rod Packing: MOF-77. In this structure (Figure 13), Zn−O−C rods are composed of tetrahedral Zn(II) centers. Four carboxyl groups that are bound in mode A bind each Zn. This connectivity pattern results in infinite Zn−O−C rods, which are cross-linked by the tetrahedral ATC link to give an arrangement where the rods propagate along *a* and *b*, resulting in a tetragonal layer packing of rods of the **ths-z** type (Table 1, Figure 1). It is worth noting that the carboxylate C atoms lie on a rod of opposite-edge-sharing tetrahedra (SiS$_2$ rod).

Strategies for the Logical Synthesis of Rod SBUs. Here, we discuss some points that should be considered when attempting to produce structures with rod SBUs. The M−O−C

SBUs of MOFs can generally be formulated $[O^0{}_a O^{1-}{}_b O^{2-}{}_c M^{n+}{}_d] (RCO_2{}^-)_e$. Here, O^0 refers to O fully bonded as in H_2O and O^{1-} refers to species such as OH^-. The condition for neutrality is $b + 2c + e = nd$. A key parameter is the O/M ratio $r = (a + b + c + 2e)/d$ because it is primarily what controls the dimensionality of the SBU. For example, in an octahedral SBU $[M^{3+}](RCO_2{}^-)_3$, we have a neutral unit with $r = 6$. For octahedral coordination, this must correspond to an isolated (finite) unit. For an infinite SBU consisting of condensed MO_6 octahedra (corner, edge, or face sharing), r must be ≤5. We can reduce r to 5 by either (a) replacing $RCO_2{}^-$ by OH^- making a basic salt as in MIL-53 described above,[10] or (b) by replacing $RCO_2{}^- + M^{3+}$ by $O^{2-} + M^{4+}$ again making a basic salt (MIL-47),[8] or (c) by replacing $RCO_2{}^- + M^{3+}$ by $O^0 + M^{2+}$ using a neutral species to complete the coordination shell as in MOF-71.

For the MOF-5 SBU $OZn_4(RCO_2)_6$, $a = b = 0$, $c = 1$, $d = 4$, $e = 6$, and $n = 2$.[1a] The parameter $r = 13/4$ (3.25). If the Zn atoms are in tetrahedral coordination, then for an infinite SBU consisting of ZnO_4 condensed (corner, edge, or face sharing) tetrahedra r must be ≤3. Accordingly, to convert from this finite SBU to an infinite SBU with tetrahedra coordination, one must again decrease the value of r. This can be accomplished by replacing one $RCO_2{}^-$ by O^- (e.g., OH^-) or 2 $RCO_2{}^-$ by O^{2-}, that is, by making a more basic salt. However, when this is attempted by adding small amounts of base and water to
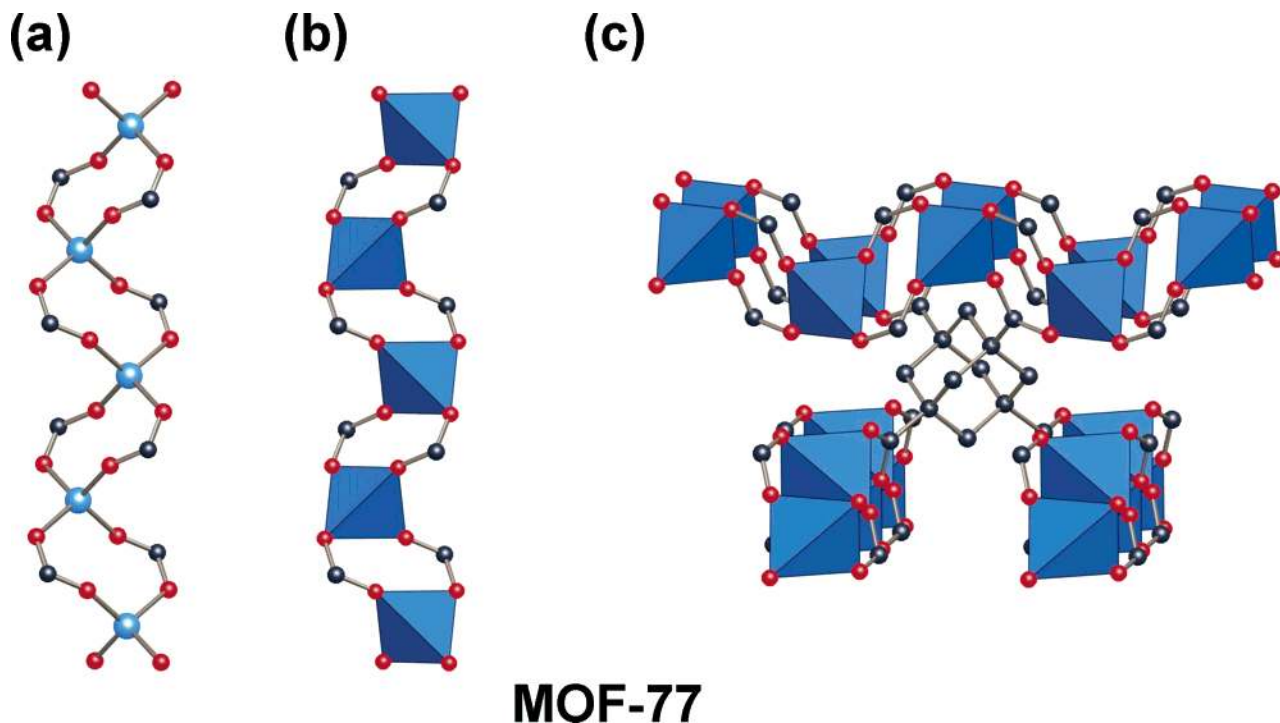
MOF-77

Figure 13. MOF-77: ball-and-stick representation of SBU (a); SBU with Zn shown as polyhedra (b); view of crystalline framework with inorganic SBUs linked together via tetrahedron of adamantanetetracarboxylate (c). All drawing conditions are the same as in Figure 3, with Zn in blue.

reactions known to produce the MOF-5 SBU, we obtain the infinite SBU found in MOF-69 with mixed octahedral and tetrahedral coordination.[3] This new SBU can formally be derived from that of MOF-5 by the following process:

$$3OZn_4(RCO_2)_6 + 2OH^- + 3H_2O \rightarrow$$
$$4(OH)_2Zn_3(RCO_2)_4 + 2RCO_2^-$$
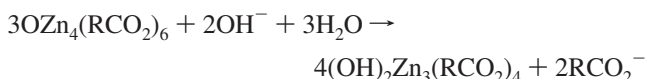
Here, *r* has increased from 13/4 (3.25) to 10/3 (3.33) as a consequence of the higher average coordination number of Zn^{2+} (i.e., 4 ZnO_4 in MOF-5 to 2 ZnO_4 and 1 ZnO_6 in MOF-69). These conditions will not produce an infinite condensed SBU with only tetrahedral Zn, but it turns out that $1/3$ of the Zn atoms are in octahedral coordination and part of an infinite SBU. Indeed, this indicates that infinite SBUs will be favored for higher coordination (see, e.g., MOF-70).

It is worth mentioning that we do not claim at this stage to be able to design the M–O–C SBU a priori; instead, we are claiming that we can identify variables and strategies for producing a particular kind of SBU. Once we know the conditions under which a given SBU can be prepared, we can then combine it with a variety of organic linkers to produce a wide range of structures as we have done for literally dozens of compounds with, for example, the copper paddle-wheel[16] and the basic zinc acetate SBU.[1a–c,17] The isoreticular series of MOF-

(16) For a systematic account of linking Cu carboxylate paddle wheels, see: (a) Eddaoudi, M.; Kim, J.; Vodak, D.; Sudik, A.; Wachter, J.; O'Keeffe, M.; Yaghi, O. M. *Proc. Natl. Acad. Sci. U.S.A.* **2002**, *99*, 4900–4904. Other MOF examples are: (b) Chui, S. S.-Y.; Lo, S. M.-F.; Charmant, J. P. H.; Orpen, A. G.; Williams, I. D. *Science* **1999**, *283*, 1148–1150. (c) Chen, B.; Eddaoudi, M.; Reineke, T. M.; Kampf, J. W.; O'Keeffe, M.; Yaghi, O. M. *J. Am. Chem. Soc.* **2000**, *122*, 11559–11560. (d) Chen, B.; Eddaoudi, M.; Hyde, S. T.; O'Keeffe, M.; Yaghi, O. M. *Science* **2001**, *292*, 1021–1023.
(17) Chae, H. K.; Kim, J.; Delgado-Friedrichs, O.; O'Keeffe, M.; Yaghi, O. M.. *Angew. Chem., Int. Ed.* **2003**, *42*, 3907–3909.
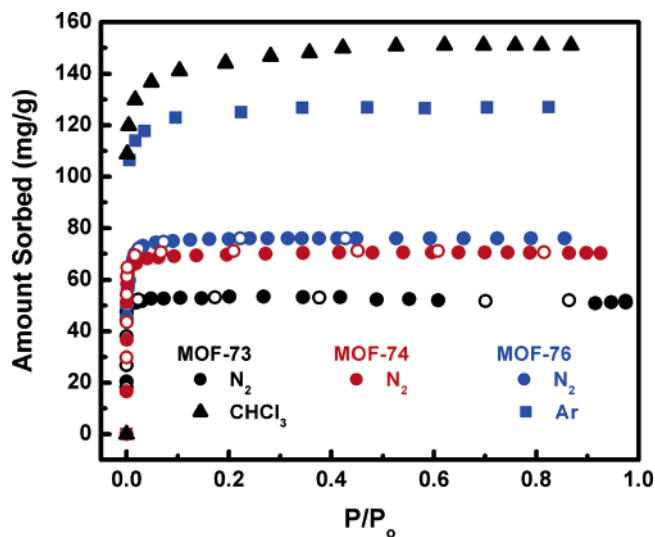

Figure 14. Gas sorption isotherms for MOF-73, MOF-74, and MOF-76. For the nitrogen isotherms, the open circles represent desorption.

69A, MOF-69B, and MOF-69C reported here is another example of a successful implementation of this strategy applied now to an infinite SBU.

Porosity and Architectural Stability of 3-D Rod-Containing Frameworks. To determine whether the MOFs constructed from rod SBUs can maintain their structural integrity in the absence of guests, we examined the gas sorption behavior of the most open members of this series: MOF-73, -74, and -76. These materials were evacuated by either heating to remove terminal DEF ligands pointing into the pores (MOF-73) and DMF guests (MOF-76), or exchanging terminal DMF ligands with water and ethanol, followed by heating to remove the ethanol and the water guests (MOF-74). In all three cases, the

Table 3. Sorption and Molecular Sieving Data for MOF-76[a]

evacuation temperature (°C)	sorbate	amount sorbed (mg/g)	pore volume (cm³/g)	Langmuir surface area (m²/g)
120	N_2	76.01	0.094	264
120	Ar	126.9	0.094	
200	N_2	98.00	0.121	334
200	CH_2Cl_2	243.59	0.184	
200	C_6H_6	144.85	0.165	
200	C_6H_{12}	95.1	0.130	

[a] Sieving is with organic solvents after activation at 200 °C.

evacuated materials reversibly sorb $N_{2(g)}$ and all isotherms are of Type I class (Figure 14), indicative of permanent microporosity and architectural stability of their evacuated frameworks. Similar behavior was observed for $Ar_{(g)}$ uptake into MOF-76 and organic vapors into MOF-73 and MOF-76.

Molecular Sieving by MOF-76. It is worth noting that because the pores in MOF-76 are one-dimensional and sorption at low temperature is mostly controlled by diffusion, the N_2 (kinetic diameter: 3.65 Å) and argon (3.4 Å) sorption reveals a lower sorption uptake as compared to a favored sorption of CH_2Cl_2 at room temperature. Similar findings were documented for zeolite sorption studies and are attributed to possible obstruction within the channels that are amplified at lower temperatures.[18] In this case, the sorption is sensitive to the applied activation temperature of evacuation because an uptake increase was observed upon activation at 200 °C as compared to the prior activation at 120 °C. The evacuated TbBTC framework showed molecular sieving, and the data are summarized in Table 3. These data are in agreement with the expected trend based on radii of adsorbate, given the corre-

(18) Breck, D. W. *Zeolite Molecular Sieves*; John Wiley & Sons: New York, 1974.

sponding radii of the adsorbates (cyclohexane, 6.20 Å; methylene chloride, 4.00 Å; and benzene, 5.85 Å).

Summary and Conclusions

This contribution outlined the principles for constructing structures from rodlike building blocks and identified the most likely nets that should result from the combination of metal–carboxylate rods with organic linkers. We demonstrated the success of this approach by linking rods with organic units to produce 14 new MOF structures with rigid and porous architectures that are based on four different rod packing nets. It was shown that most MOF structures are based on parallel rod packings; however, the rod and link metrics required to make new MOFs adopting more complex rod packing have also been presented. They point toward a strategy for preparing structures based on 3- and 4-way rod packings; such structures are expected to have greatly enhanced stability due to the three-dimensional nature of the packing. Finally, we recall this is the first extensive effort to prepare such structures, and as experience is gained with controlling the formation of rods of certain types, attention can be directed toward controlling the type of rod packing.

Supporting Information Available: Data collection, structure solutions, refinement parameters, and ORTEP diagrams for MOF-69−80 and CIF files for MOF-69−80. This material is available free of charge via the Internet at http://pubs.acs.org.

JA045123O